4

Physical properties of wool

J W S HEARLE

4.1 The wool fibre

4.1.1 Structural complexity

As is clear from Chapter 3, wool and other hair fibres have the most complicated structures of all textile fibres. All of the many levels of structure described in Chapter 3 have an influence on the physical properties of the fibres, and the mechanisms are now mostly understood qualitatively and, in many parts, supported by quantitative analysis. For convenience, the wool structure is summarised in Fig. 4.1, which is similar to Fig. 3.2 but emphasises aspects that are relevant to a discussion of the physical properties of fibres.

4.1.2 Dimensional and other features

An idealised wool fibre has a circular cross-section, with diameters for different wools covering a range that can roughly be put as 20 to 40 μm. In reality, the cross-section is slightly and imperfectly elliptical. Fibre lengths range roughly from 5 to 50 cm. The fibres are helically crimped to varying degrees. The differences between different wool types and the methods of measuring dimensions are discussed in Chapter 1. In general, this Chapter will deal with generic features of wool fibres and will not cover differences between different wools.

The density of wool is 1.3 g/cm^3. The refractive indices of wool are reported[1] as 1.553 parallel to the fibre axis, 1.542 perpendicular, and a birefringence of 0.010.

4.2 Effects of water

4.2.1 Moisture absorption

The proteins in wool contain —CO.NH— and other groups that attract water. Figure 4.2 shows the change in moisture regain (mass of absorbed

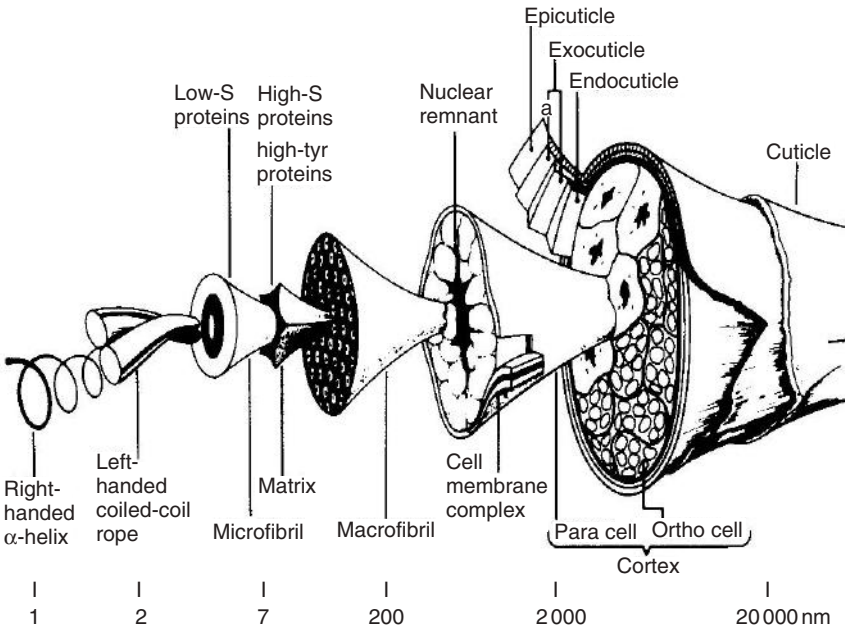

4.1 Wool fibre structure. Note that many wool fibres have a meso-cortex, as well as ortho- and para-cortex, and in some coarse wools there is a medulla. [*Drawn by Robert C Marshall, CSIRO.*]

water/mass of dry fibre) with relative humidity.[2] In a standard atmosphere of 65% RH and 20 °C, regain values range from 14 to 18%. Preston and Nimkar[3] found that loose wool retained 133% regain when suctioned at –30 cm of mercury from the wet state but only 45% when centrifuged at 1000 g for 5 minutes. This contrasts with other fibres where the two methods give similar values.

As can be seen in Fig. 4.2, there is hysteresis in moisture absorption, with the desorption curve being higher than the absorption curve. The shorter intermediate curves show the changeover from absorption to desorption at different humidities. Regain at a given relative humidity varies with temperature; at 70% RH, Darling and Belding[4] found values between 17 and 18% from –29 °C to 4 °C, but then it fell to 13% at 71 °C.

There have been a number of thermodynamic and mechanistic theories of moisture absorption in wool.[5] There is general agreement that the sigmoidal shape of the absorption curve is a combination of water directly held on hydrophilic sites in the protein molecules, which increases rapidly from zero relative humidity and then levels off, and more loosely held water, which increases rapidly at high humidiites. Speakman[6] divides the absorption into three types as shown in Fig. 4.3. The first type (a) is

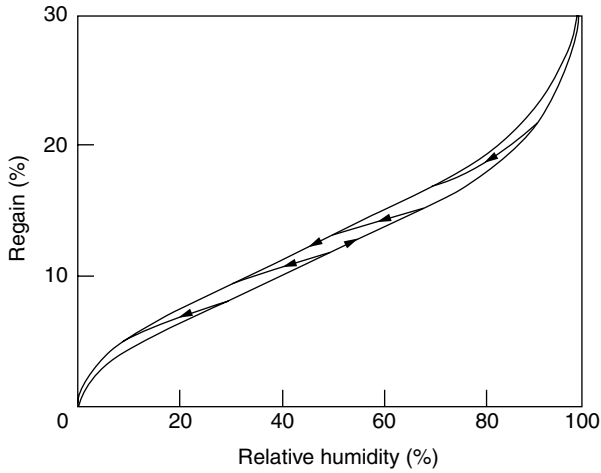

4.2 Change of moisture regain of wool with humidity. [*After Speakman et al.*[2]]

assumed to be bound to hydrophilic groups in protein side-chains, and has little effect on torsional rigidity or, according to Hearle,[7] on dielectric constant and electrical resistance. The second type (b) is attached to groups in the main chain, where it replaces intermolecular hydrogen bonds, and is linearly related to rigidity. The third type (c) is absorbed on top of types (a) and (b).

When wool takes up water, the swelling is almost entirely radial, with little change in length. The overall volume increases, initially by a lower amount than the volume of absorbed water, but above about 15% regain the volumes are additive. Table 4.1 shows a set of values for radial and volume swelling, together with the change in fibre density.[8]

The swelling behaviour is explained on the presumption that most or all of the water is absorbed by the matrix, due to the presence of accessible hydrophilic groups, and that this increases the lateral spacing between fibrils, whose length does not change. The first molecules to be absorbed can pack efficiently with the protein molecules, but the later ones merely increase the volume.

4.2.2 Heat of sorption

Table 4.2 gives values for the heat of wetting of wool, namely the amount of heat evolved when the wool is completely wetted out from different regains.[8] From this, the differential heat of sorption, namely the heat evolved when one gram of water is absorbed, is calculated. The initial bonding of water to hydrophilic groups generates a large amount of

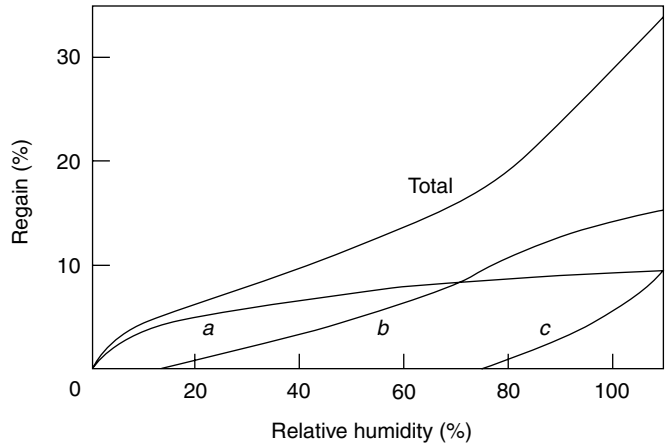

4.3 Absorption of water in three types. [*After Speakman.*[6]]

Table 4.1 Moisture absorption and swelling of wool [From: WIRA[8]]

Moisture regain (%)	0	2	5	7	10	15	20	25	30	33
Approximate RH (%)	0	2.5	15	27	42	68	85	94	98.5	100
Radial swelling (%)	0	0.66	1.82	2.62	4.00	6.32	8.88	11.7	14.6	16.3
Volume swelling (%)	0	1.57	4.24	6.10	9.07	14.3	20.0	26.2	32.8	36.8
Density (g/cm^3)	1.304	1.310	1.314	1.315	1.315	1.313	1.304	1.291	1.277	1.268

heat, but near saturation the effect is small. It has been found that the differential heat of sorption H follows equation [4.1], which is based on Kirchoff's equation for dilution of solutions. This is expressed in terms of the relative humidities, h_1 and h_2, at temperatures, T_1 and T_2, for a constant regain:

$$2.3 \log(h_1/h_2) = 9\ H(1/T_2 - 1/T_1) \qquad [4.1]$$

The values in Table 4.2 are for take-up of liquid water. For absorption of water vapour, the latent heat of condensation (2450 kJ/kg at 20 °C), which is three times the maximum heat of sorption from liquid water, must be added to the values. This evolution of heat has an important influence in clothing. When 1 kilogram of wool is taken from 40 to 70% RH, 160 kJ of

Table 4.2 Heat of absorption of wool from liquid water [From: WIRA[8]]

Regain (%)	0	5	10	15	20	25	30	33
Approximate RH (%)	0	15	42	68	85	94	98.5	100
Heat of wetting (kJ/kg)	101	64.5	38.1	20.5	10.0	4.19	1.13	0
Diff'l heat of sorption (kJ/kg)	854	624	431	276	159	100	41.9	33.5

heat are evolved. The main effect of this is to slow down the impact of moving between hot dry atmospheres indoors and cold damp atmospheres outdoors.

4.3 Observed mechanical properties

NOTE: *Much of the data in the literature is reported as conventional stress, based on area, in N/mm^2 = MPa or, for older work, in dyne/cm^2 = 0.1 Pa. Generally, in the textile literature, it is preferable to use specific stress, namely (force/linear density) based on fibre mass. For wool, assuming a density of 1.3 g/cm^3, 1000 MPa = 0.77 N/tex, 7.7 cN/dtex or 7 g/den. Stresses are also often normalised in terms of the tension at 15% extension in wet wool, which is the middle of the yield region; this is typically around 35 MPa (27 mN/tex or 0.25 g/den).*

4.3.1 Load–extension properties

The most extensive study of the mechanical properties of wool was carried out by Max Feughelman and his colleagues at CSIRO Ryde[9] from the 1950s onwards. A special feature of their work is that, provided the fibre is not strained by more than 30% or for longer than 1 hour, it can be returned to its virgin state by soaking in water at 52 °C for 1 hour, so that many tests can be made on one fibre. Most of their tests were on fibres from sheep housed and fed in controlled conditions. These factors reduce the problems of variability within and between fibres. Figure 4.4 shows a typical load–extension curve of a wet wool fibre. The features of the curve are: (i) a low-stress decrimping extension near A; (ii) an initial stiff region up to B, usually referred to as the Hookean region – but, though linear, it is visco-elastic, not elastic; (iii) a yield region up to C; (iv) a stiffer region up to break at D. In tests on different fibres, there is little variation in the points B and C at 2% and 30% extension respectively, but the break extension varies more widely, since it is less if there is any weakness or damage in the fibre. Break extensions of 50 to 60% are typical of a good fibre. From the

start of the yield region, there is a progressive loss of the X-ray diffraction pattern corresponding to the α-helix and a growth of the pattern for the extended β-chains.[10]

Variability along the fibre length changes the shape of the curve, because thin portions extend more easily than thick portions. Consequently, part of the fibre may be suffering high extension in the yield region, while other parts are still in the Hookean region and only yield at a higher load. These features were studied in detail by Collins and Chaikin,[11] and Fig. 4.5 illustrates the stress–strain curves of fibres that are more or less regular. Their theoretical calculations[12] indicate that a perfectly uniform fibre would have a constant yield stress, i.e. zero slope between B and C in Fig. 4.4, and that the changes of slope at B and C would be sharper than are usually found. If the change in cross-section along the fibre is continuous, the effect is to give a higher yield slope, but, if it is discontinuous, there will be steps in the yield region.

Figure 4.6 shows how the stress–strain curve changes with humidity and temperature.[13] As the wool becomes drier, the main effects are to raise the yield stress, and there is some increase in yield slope. The initial modulus decreases with increasing moisture regain, as shown in Fig. 4.7.[14] It has been

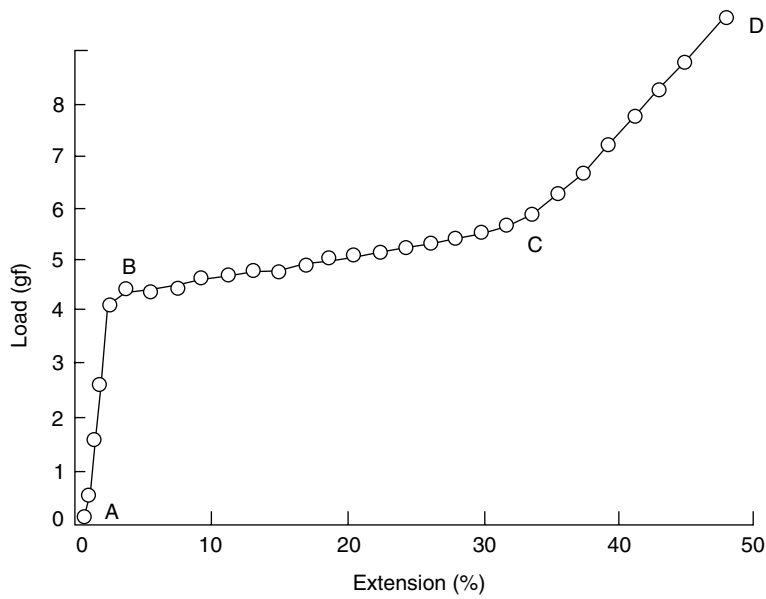

4.4 Load–extension curve of a Corriedale wool fibre in water at 20 °C. AB is the Hookean region, BC the yield region, and CD the post-yield region. Up to B, the rate of extension was 0.375% per hour, and beyond B, 1.875% per day; the whole test took 25 days. [*From Feughelman.*[9]]

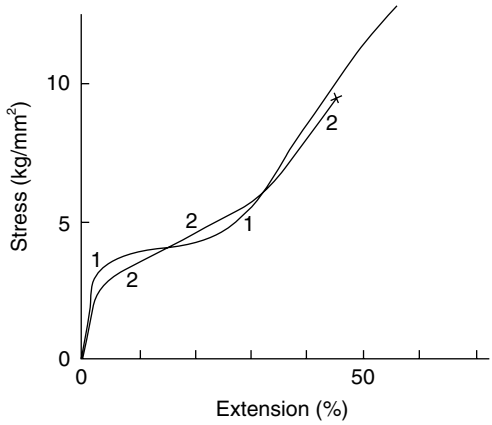

4.5 Stress–strain curves of wool fibres: (1) with good uniformity; (2) a more irregular fibre. [*From Collins and Chaikin.*[11]]

noted[15] that although the change to the yield region occurs at higher strains in drier fibres, it is at the same fibre *length* as at 100% RH, indicating that the additional extension is due to axial shrinkage of the fibre on drying, with some compression of the internal structure. Strength increases in line with the increase in yield stress, but to a lesser extent because of a reduction in break extension. An increase in temperature lowers the stress over the whole curve, with a large change between 40 and 80 °C. The shape of the curve is markedly different at 100 °C (Fig. 4.8).

The stress–strain curve is affected by the chemical environment. Figure 4.9(a) shows the effect of alcohols. Because the molecules are larger, they do not cause as much lowering of the stress–strain curve as water. The higher the alcohol, the higher is the stress, with an effect similar to reduction of humidity. Acids inherently tend to lower the stress–strain curve, as shown by formic and acetic acids in Fig. 4.9(b), but this is counterbalanced by the difficulty of the larger acid molecules penetrating the fibre.

4.3.2 Recovery behaviour

The shape of the stress–strain curve of wool in extension is not unusual for polymers, though the changes at B and C are particularly sharp. The recovery behaviour is completely different; in most polymers there is no recovery from yielding. In wet wool, as shown in Fig. 4.10, there is complete recovery from extensions up to 30%, but the recovery follows a different curve and only joins the extension curve at about 1/3 of the yield stress. In the post-yield region above 30%, the recovery curve has a similar shape,

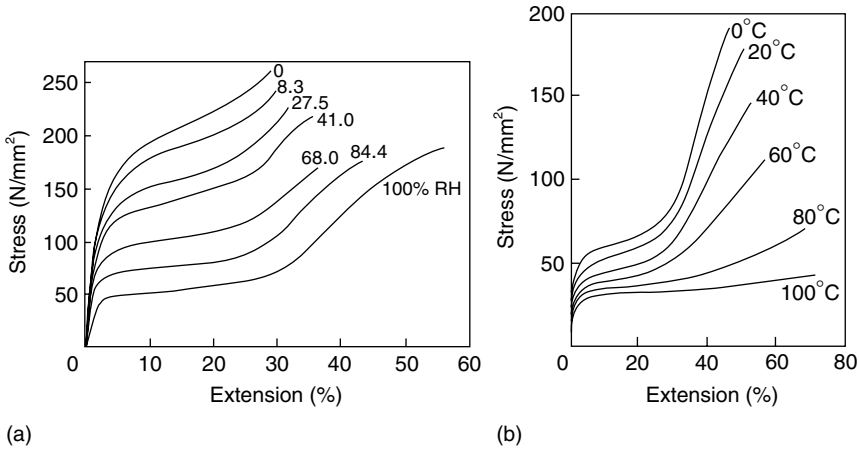

4.6 Change of stress–strain curves with test conditions:[13] (a) influence of moisture at room temperature; (b) influence of temperature for wet wool.

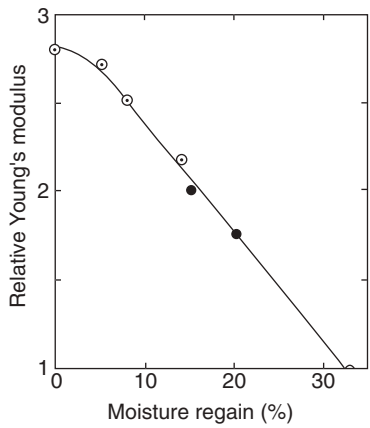

4.7 Change of initial modulus with regain. [*From Peters and Woods.*[14]]

but at zero stress there is a small unrecovered extension, which increases with the imposed extension.

In his extensive tests at 65% RH, Meredith[16] found that the elastic recovery of wool decreased with increasing imposed extension. From 30% extension, the elastic recovery (recovered extension/imposed extension) was 0.6. Table 4.3 gives other recovery data, showing the effect of humidity and imposed extension.[17]

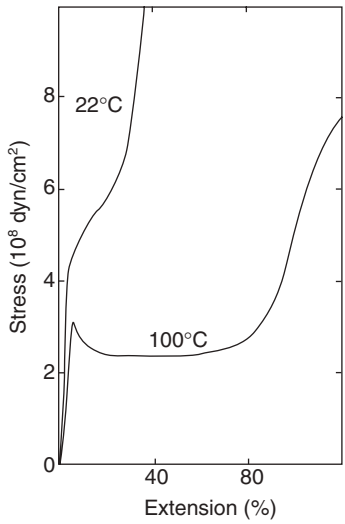

4.8 Stress–strain curves of wet wool at 22 and 100 °C. [*From Peters and Woods.*[14]]

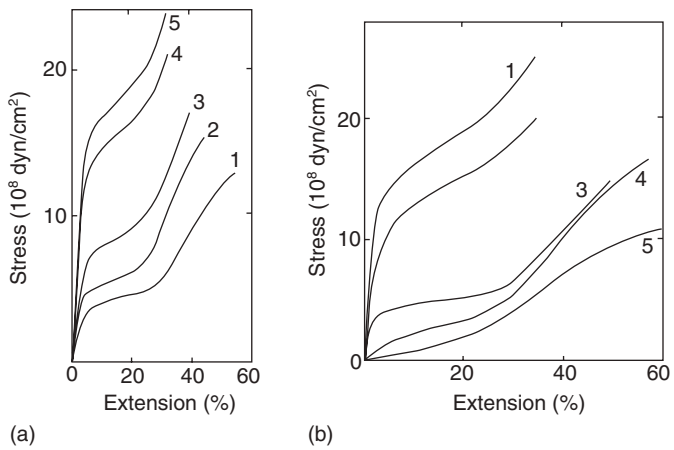

4.9 Effect of chemicals on stress–strain curves. (a) 1 – water, and alcohols, 2 – methyl, 3 – ethyl, 4 – n-propyl, 5 – n-butyl or n-amyl. (b) 3 – water, and acids 1 – n-butyric, 2 – propionic, 4 – acetic, 5 – formic. [*From Peters and Woods.*[14]]

4.3.3 Time dependence

Wool fibres contain many bonds sensitive to time under load, so that visco-elasticity shows up in reduced stress as rate-of-extension is decreased, in creep under constant load, in stress relaxation at constant extension and in changes in dynamic properties.

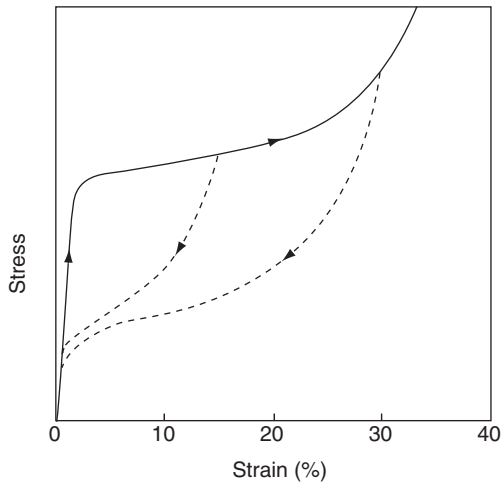

4.10 Stress–strain curve of wet wool in extension and recovery. The stress is in arbitrary units. [*From Morton and Hearle*.[5]]

Table 4.3 Elastic recovery of wool [From: Beste and Hoffman[17]]

Humidity	Elastic recovery from extension of		
	1%	5%	10%
60% RH	99%	69%	51%
90% RH	94%	82%	56%

In the low-strain Hookean region, Fig. 4.11, from studies by Feughelman and Robinson,[18] shows that the higher stress at lower humidities relaxes with time towards the stress in the wet state. From larger strains, Fig. 4.12 shows the stress relaxation of human hair, which will be generally similar to wool, from different extensions in water at 35 °C and from 40% extension at different temperatures.[14] The curves divide into four regions, which shows that there are different relaxation mechanisms within the fibre structure. There is rapid decay in less than a second, which, if it were the only mechanism, would lead to an asymptotic approach to a limiting tension. This is followed by a slow decay to 100 seconds, then a faster decay from 100 to 10 000 seconds, before the curve begins to flatten out. The increase in rate at higher temperatures is also shown in Fig. 4.13 for relaxation from the mid-point of the yield region.[19]

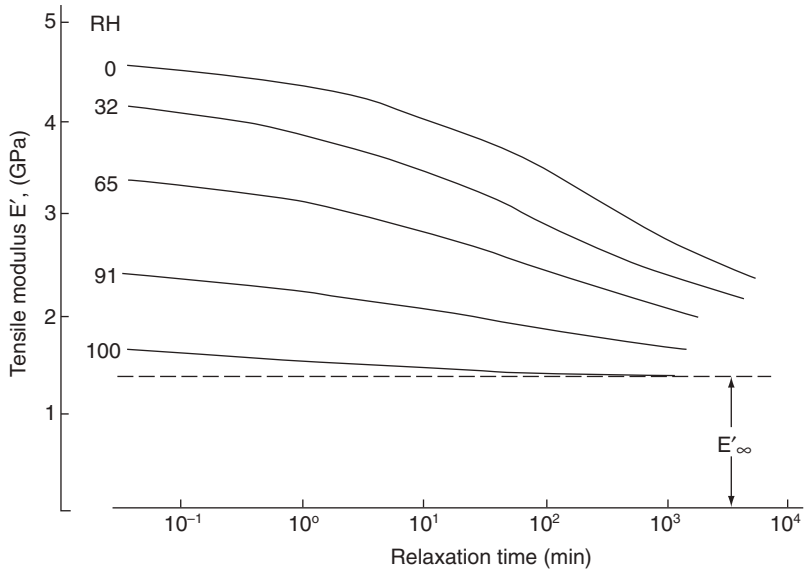

4.11 Stress relaxation of a wool fibre from 0.8% extension at different relative humidities.[18] The stress, calculated on the basis of the wet cross-sectional area, is normalised to the stress at 0.8% extension in a wet fibre. [*From Postle et al.*[26]]

Figure 4.14 shows the creep in a wet wool fibre for short times (2.5 minutes) under different loads in the yield region at 18.5 °C and in the yield region at different temperatures.[20] The rate decreases with time and, on a linear time scale, appears to become asymptotic to a constant value. Creep is faster at higher temperatures. Feughelman[20] found that the results fitted the empirical equation:

$$1/e = (a/t) + b \qquad [4.2]$$

where e is extension at time t, and a and b are constants dependent on load and temperature.

When tested over longer times and plotted on a logarithmic scale, Fig. 4.15 shows that another mechanism appears to take over at around 100 minutes and begins to level off in a typical sigmoidal plot at about one week.[18]

The creep, or stress relaxation, in wool will show up as higher extensions at a given stress in load–extension testing. Figure 4.16 shows the effect on Young's modulus, which decreases as the rate of extension is decreased.[18]

As can be seen in Fig. 4.17(a), the dynamic modulus, measured by small oscillations at 116 Hz,[21] is highest at a small mean strain level in the Hookean region, is lower through the yield region, and rises again in the post-yield

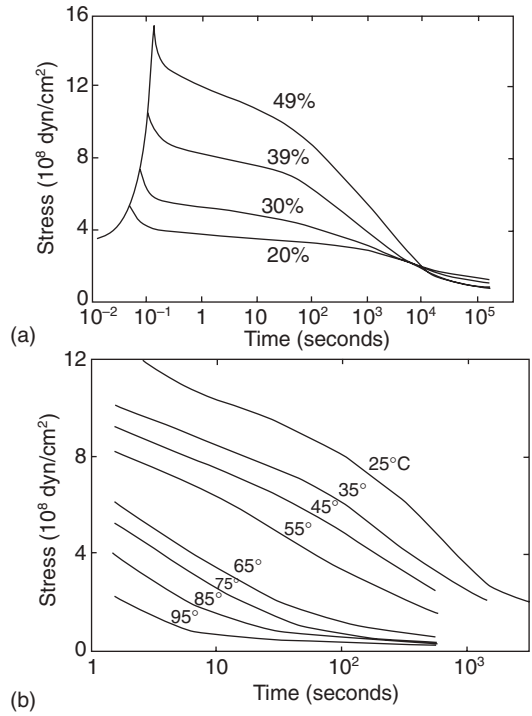

4.12 Stress relaxation of wet human hair: (a) at 35 °C from different extensions; (b) from 40% extension at different temperatures. [*From Peters and Woods.*[14]]

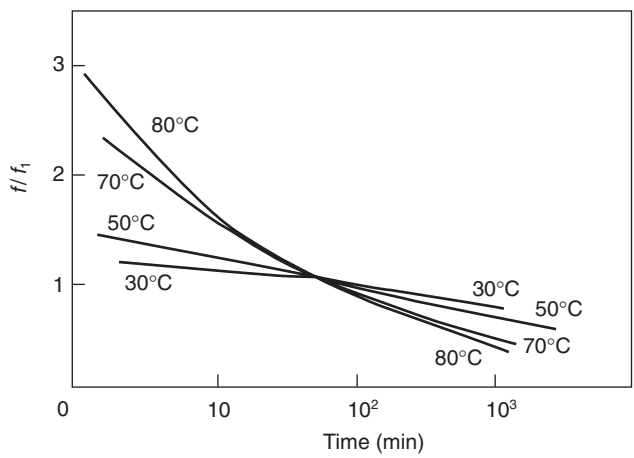

4.13 Relaxation of wet wool from 15% extension at different temperatures.[19] f/f_1 is the ratio of the stress after the given time to the stress after 1 hour. [*From Morton and Hearle.*[5]]

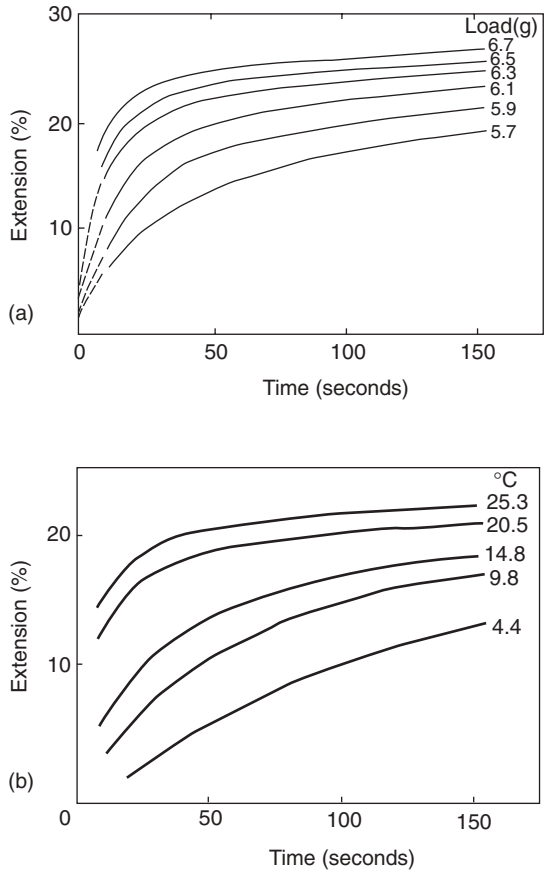

4.14 Creep in a wet wool fibre with a diameter of 44.5 μm:[20]
(a) under various loads at 18.5 °C; (b) under 6 gram load at various temperatures. Note that 6 gram equals 38.5 MPa, which is towards the end of the yield region.

region. Conversely, the plots of loss angle δ in Fig. 4.17(b) are roughly mirror images of the modulus plots, being highest in the yield region. Figure 4.18 shows the change in tan δ in dry fibres with temperature, as measured by Meredith in bending.[22] For wool, there is a rise, presumably to a peak characteristic of many polymers around –100 °C, at low temperature; a peak at about 20 °C; and then a rise at high temperature.

4.3.4 Directional effects

The bending behaviour of fibres relates to their tensile properties, with the outside of the bend being in tension and the inside in compression. For

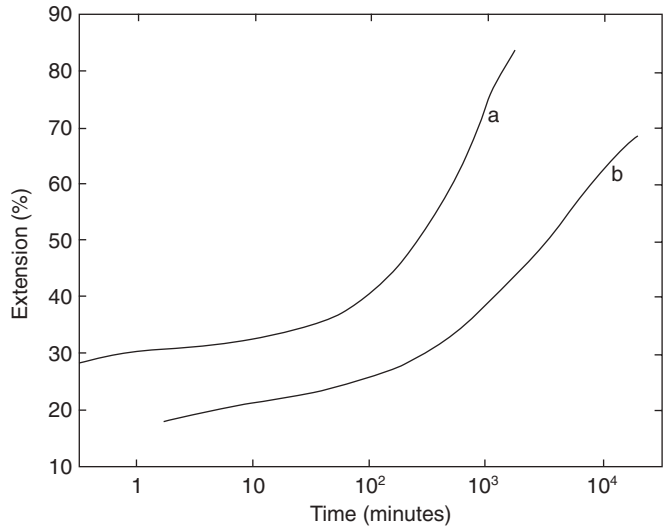

4.15 Creep of keratin fibres in water: (a) human hair at 72 MPa; (b) Cotswold wool at 69 MPa. [*From Peters and Woods.*[14]]

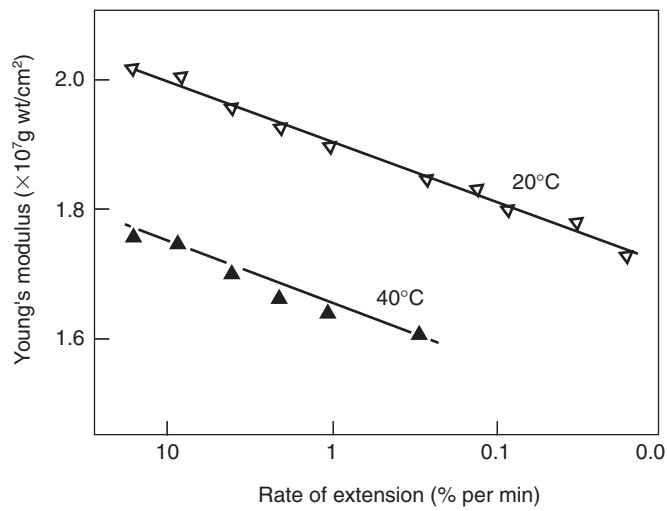

4.16 Change of Young's modulus in wet Cotswold wool with rate of extension at 20 °C and 40 °C.[18] [*From Morton and Hearle.*[5]]

small curvatures with a constant modulus, there is a central neutral plane and the maximum strain is $\pm(r/R)$, where r is the fibre radius and R is the radius of curvature. If there is yielding, the neutral plane is displaced in order to minimise the deformation energy. In most polymers, yielding is

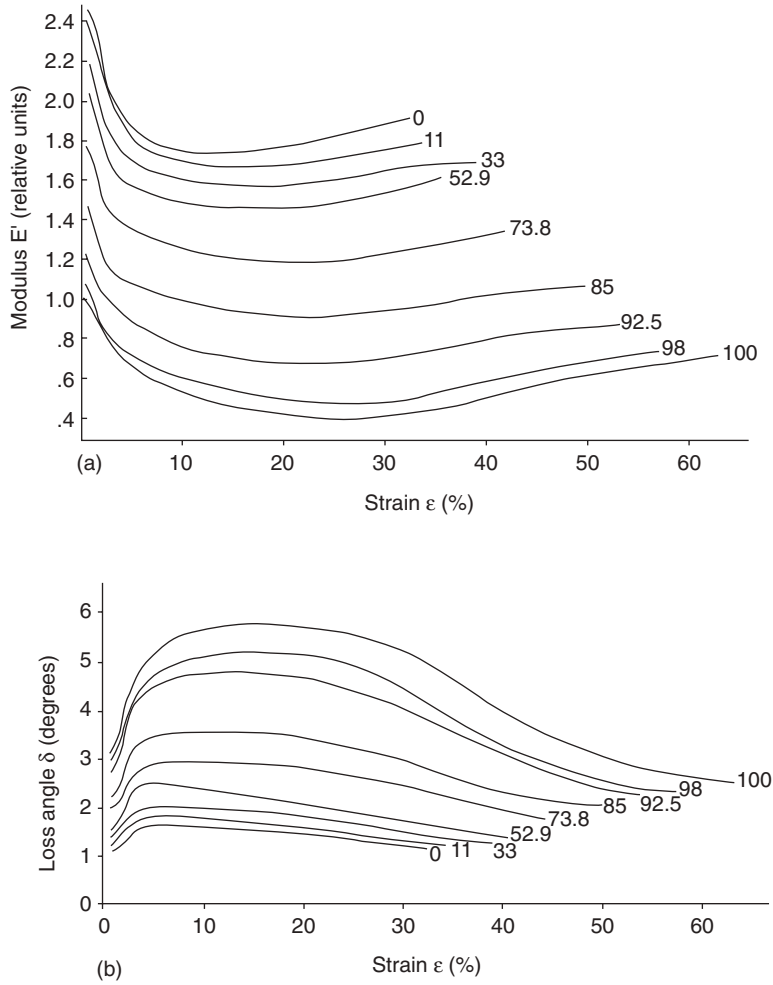

4.17 Dynamic mechanical properties of Lincoln wool at different humidities at 25 °C and 116 Hz: (a) Dynamic modulus *E′*. Unit modulus at 0.6% extension equals 2 GPa. (b) Loss angle δ. [*From Danilatos and Feughelman.*[21]]

easier in compression than extension, so that the neutral plane moves out and a plot of equivalent stress against strain in bending falls below that in extension, as found for several fibres by Chapman.[23] However, for Lincoln wool, the bending curve goes above the tensile curve, as shown in Fig. 4.19(a). Experiments up to higher curvatures on a coarser horse hair fibre show the effect of the eventual yielding in compression, Fig. 4.19(b). The initial identity of both curves shows that the tension and compression moduli are the same in the Hookean region. Figure 4.20 shows the effect

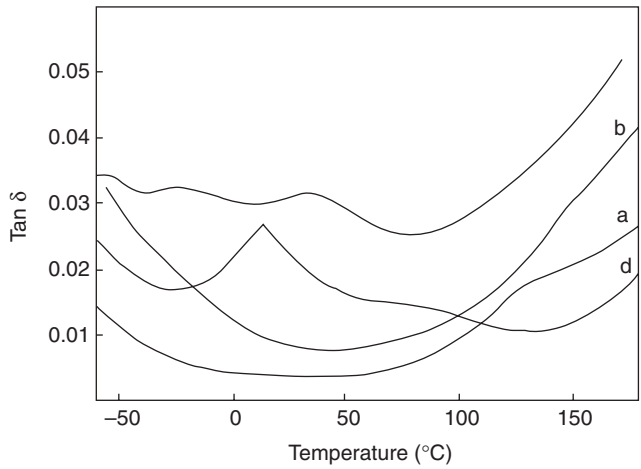

4.18 Loss factor for several fibres measured in bending by Meredith[22]. Curve (d) is for wool. The others are: (a) mercerised cotton, (b) viscose rayon, (c) secondary acetate [*From Morton and Hearle.*[5]]

of temperature and humidity on the nominal initial bending modulus: the black circles are repeats at 20 °C after tests at 60 °C; the dotted line is calculated from tensile modulus and swelling data of Bendit and Feughelman,[24] and shows good agreement despite being on different wools at different rates.

The changes in differential axial length of wool on drying, as discussed in Section 4.4.3, cause wool to bend on drying from the form in which it grows from the follicle, and this leads to the helical crimp of wool fibres.

The torsional properties of wool were measured by Mitchell and Feughelman.[25] Figure 4.21 shows that there is a linear relation between the reciprocal of torque and the reciprocal of twist angle. The resistance to twisting decreases with increasing humidity. Speakman[6] showed that the reduction in torsional rigidity followed a sigmoidal plot against moisture regain, Fig. 4.22, but was linear when plotted against the intermediate absorption, shown as type (b) in Fig. 4.3. The shear modulus, as measured in torsion, is reported[26] to be 1.7 GPa at 0% RH, 1.1 GPa at 65% RH, and 0.13 GPa at 100% RH. The effects of temperature, strain and moisture on torsional stress relaxation are shown in Fig. 4.23.

Figure 4.24 shows the transverse load–extension curve of wet porcupine quill.[27] The initial modulus of 0.37 GPa should be valid as a measure of the properties of the material of the wool fibre, but, as suggested by Hearle,[28] the yielding is probably due to breakdown of the composite structure at some level. Kawabata has developed sensitive methods for measuring the properties of fibres in different directions. He reports the following values

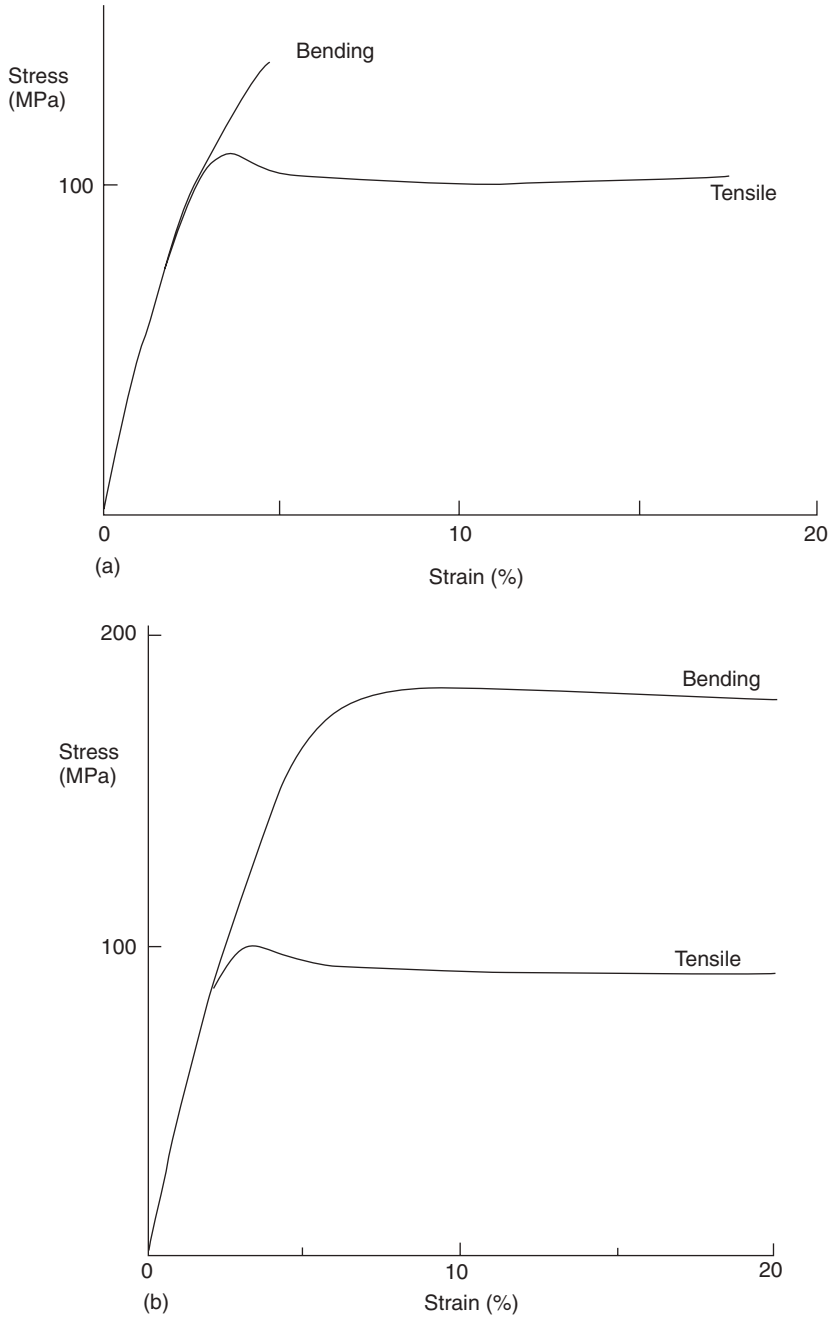

4.19 Nominal stress–strain curves in bending compared with tensile curves: (a) Lincoln wool; (b) horsehair. [*From Chapman.*[23]]

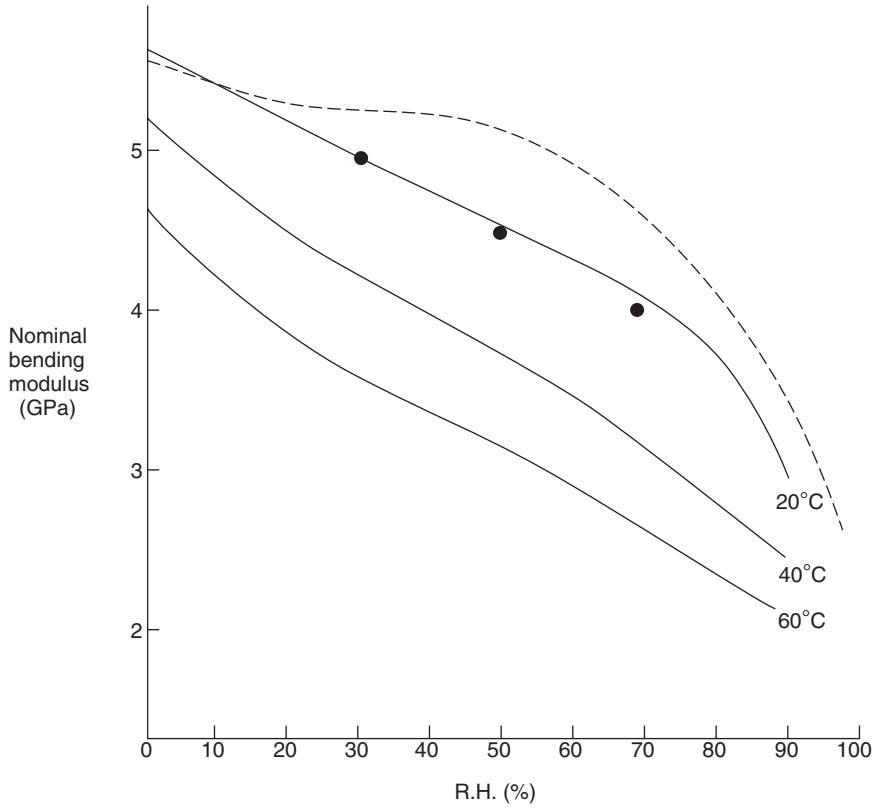

4.20 Effect of temperature and humidity on nominal bending modulus of Lincoln wool. See text for explanation of black circles and dotted line. [*From Chapman.*[23]]

at 25 °C and 55.3% RH: axial modulus E_L = 3.33 GPa; transverse modulus E_T = 1.09 GPa; shear modulus G_{LT} = 1.47 GPa.[29]

4.3.5 Fibre strength: fracture and fatigue

For 'good' wool, the evidence indicates that wet fibres break at an extension of 50 to 60% at a stress of about 100 MPa. Figure 4.25 shows a plot of break load in a standard atmosphere against the local area of cross-section at the break point of wool fibres.[30] The slope of the upper bound line indicates an intrinsic strength of 300 MPa. However, the break load of individual fibres, when related to their average diameter or linear density, may be much lower than this due to variability, which causes failure to occur at a thin place. The points falling below the line in Fig. 4.25 can be attributed to

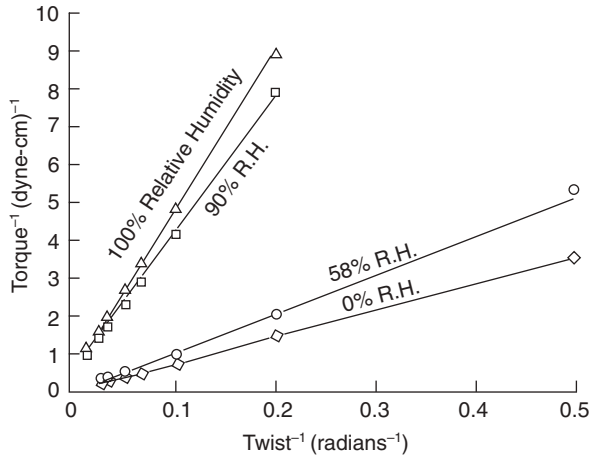

4.21 Reciprocal of torque plotted against reciprocal of twist angle for a wool fibre of diameter 44.6μm when wet.[25] [*From Feughelman.*[9]]

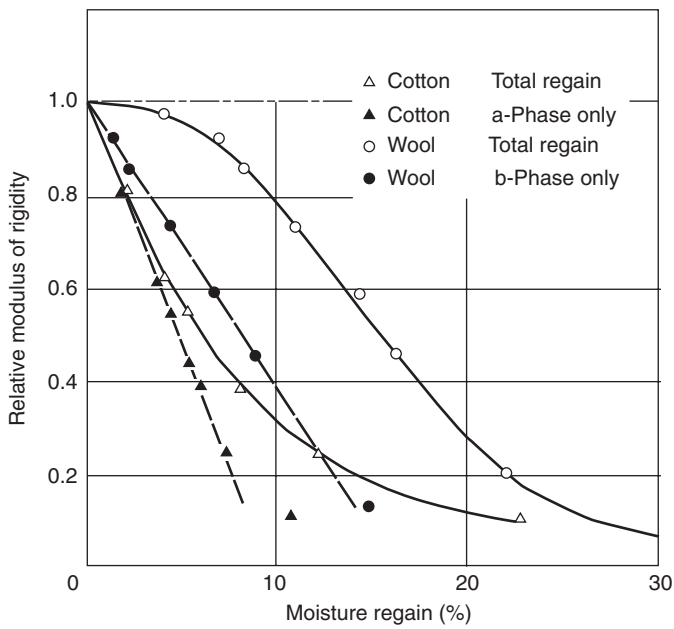

4.22 Relative torsional rigidity plotted against moisture regain. The upper plots are for wool; the comparison for cotton shows a plot against the first absorbed water in a two-phase model. [*From Morton and Hearle.*[5]]

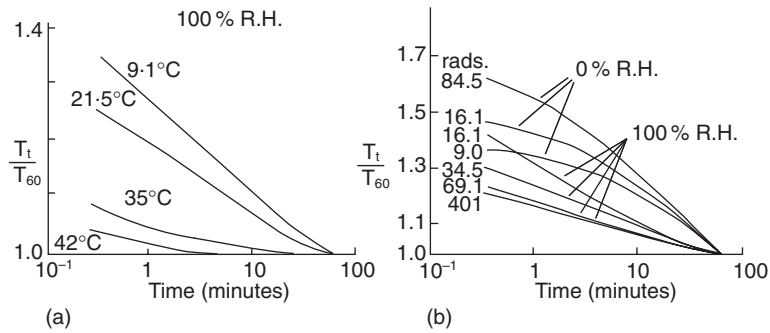

4.23 Torsional stress relaxation, plotted relative to stress after 60 minutes: (a) effect of temperature at 100% RH; (b) effect of strain at 0% and 100% RH. [*From Chapman.*[15]]

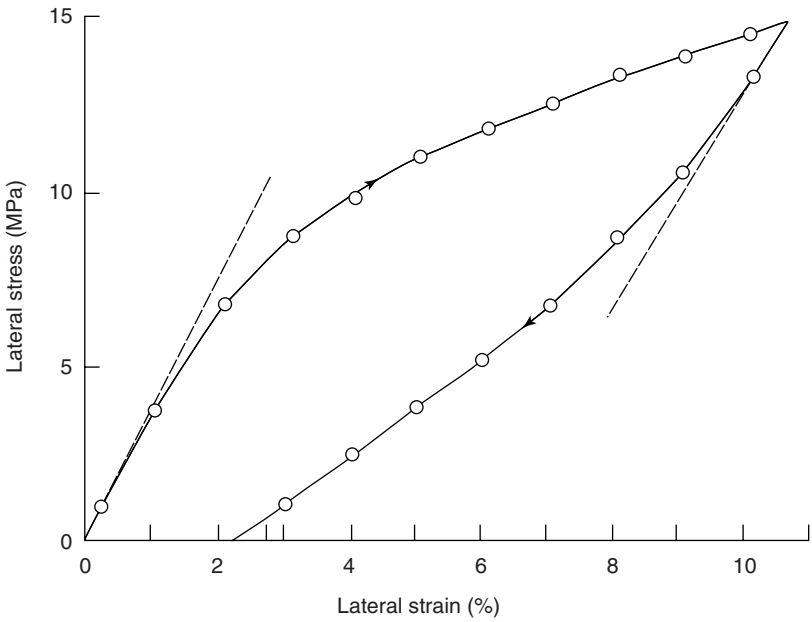

4.24 Stress–strain curve for porcupine quill in lateral extension.[28] [*From Feughelman.*[9]]

some defect in the fibre, which may be a surface crack, an internal flaw, or some general weakness in the fibre.

The form of tensile fracture is a granular break perpendicular to the fibre axis, Fig. 4.26(a).[31] In some fibres, the break is in short or long steps joined by an axial split, Fig. 4.26(b,c). The two transverse cracks are an indication

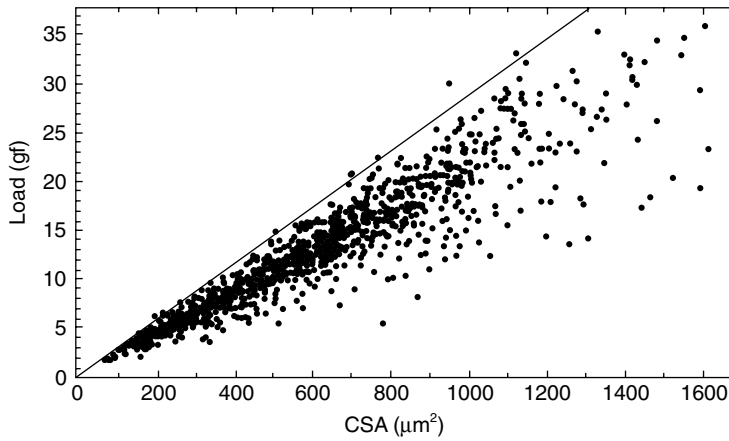

4.25 Break load of wool fibres plotted against area of cross-section at point of break.[30]

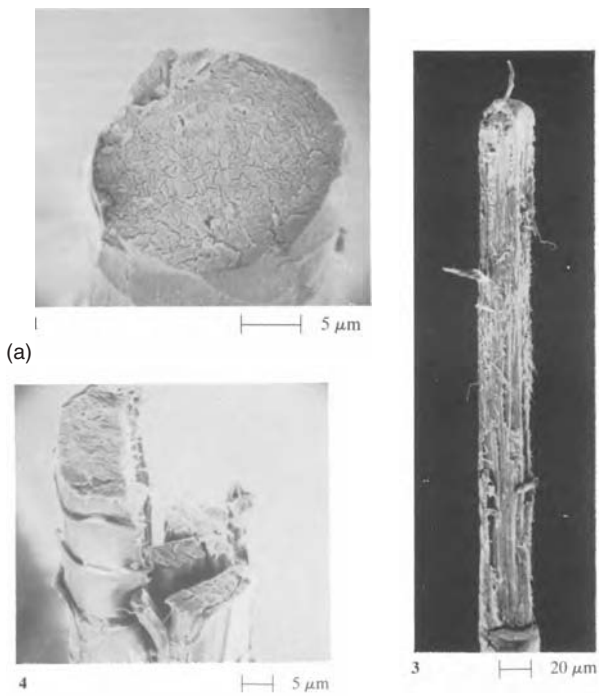

4.26 Three views of the tensile fracture of wool fibres. [*From Hearle et al.*[31]]

of prior damage to the fibre, either a pre-existing split or flaws in two places along the fibre.

When wool is repeatedly flexed by pulling to-and-fro over a pin, there is a combination of axial splitting and surface wear,[32] as shown in Fig. 4.27. Severe repeated buckling, either in a laboratory test or in a carpet, leads to the formation of axial cracks due to internal buckling in axial compression,[32] as shown in Fig. 4.28(a). This leads to rupture, Fig. 4.28(b), and is followed by axial splitting.

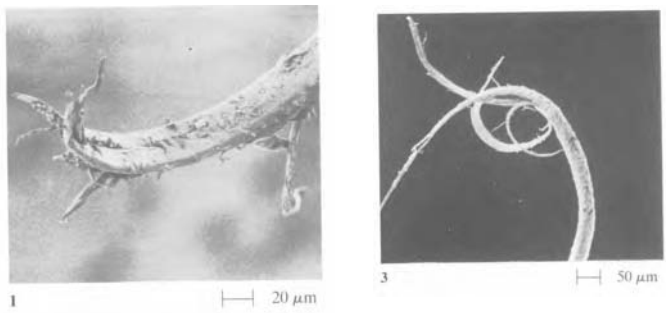

(a) (b)

4.27 Failure in wool fibres on flexing over a pin. [*From Hearle et al.*[31]]

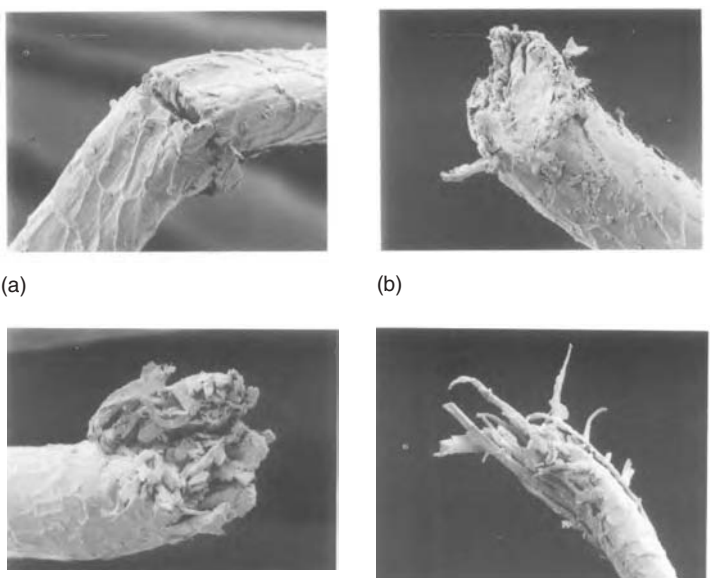

(a) (b)

(c) (d)

4.28 Failure in repeated severe buckling of a wool yarn. (a) transverse crack; (b) ruptured end; (c,d) subsequent axial splitting. [*From Hearle et al.*[31]]

4.3.6 Thermal properties, transitions, supercontraction

The thermal conductivity of horn, which is a similar material to wool, increases from 194 $mWm^{-1}K^{-1}$ at 0% moisture regain to 290 $mWm^{-1}K^{-1}$ at 30% regain.[32] For fibre assemblies, the trapped air leads to much lower values of thermal conductivity.

Figure 4.29 shows the variation of specific heat of wool with temperature at various regains.[33] The peak below 0 °C at higher regains will be due to the latent heat of 'freezing' of loosely bound absorbed water. There is also an indication of a step increase at around 40 °C, which would correspond to a second-order glass transition.

A differential scanning calorimetry study by Phillips[34] showed that the change in specific heat was considerably affected by fibre ageing. Wool with 15% regain stored at 20 °C for 52 days showed a pronounced endotherm near 60 °C on the first heating cycle, which disappeared in a second run after rapid cooling, but reappeared after 15 days reageing. Figure 4.30 shows how the transition temperature falls with increasing water content.

The effect of the second-order transition on mechanical properties is shown by the large drop in the stress–strain curve of wet wool between 40 °C and 80 °C, as seen in Fig. 4.6. The position of the transition is clearly

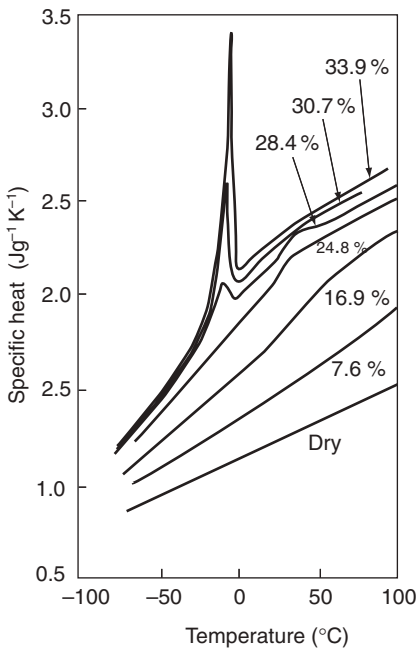

4.29 Variation of specific heat of wool with temperature and regain.[33] [*From Morton and Hearle.*[5]]

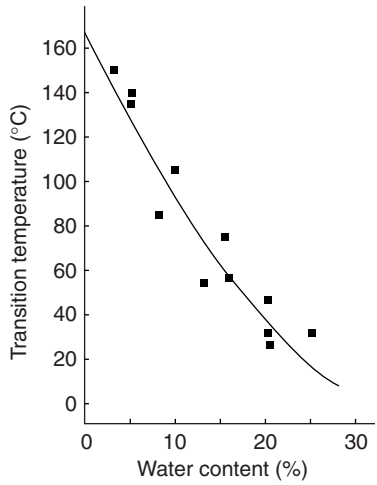

4.30 Variation of transition temperature of wool with water content. [*From Phillips.*[34]]

shown in Fig. 4.31 by the change in the strain at the end of the yield region in wet wool. There is no change up to 60 °C, but then there is a rapid increase. The plot of initial modulus against temperature shows a reduction associated with the glass transition, but it then drops rapidly above 100 °C to almost zero at 130 °C, Fig. 4.32.

The effects above 100 °C are attributed to a first-order transition and are associated with the phenomenon of supercontraction, which may be brought about in various ways. A fibre that has been stretched to above 40% extension, steamed and released, will contract to less than its original length. Irreversible supercontraction occurs when wool is immersed in a boiling solution of phenol or a lithium halide in water, and reversible supercontraction occurs in cuprammonium hydroxide or a lithium halide solution in milder conditions. In a hot solution of lithium halide, the fibre contracts in a first stage to around –15% extension, with a complete loss of crystallinity, as shown by X-ray diffraction, and of birefringence. After a few minutes, second-stage supercontraction goes to a final value between –30% and –50% extension. Washing the fibre after the first stage restores the fibre to its original state, but this does not occur after the second stage.

First-stage supercontraction occurs after many hours in a cold lithium bromide solution above a critical concentration; second-stage supercontraction occurs when the concentration is increased and heat is applied. Chapman[35] used this procedure to investigate the change in tensile properties. Figure 4.33 shows the stress–strain curves in water and in cold LiBr solution after first- and second-stage supercontraction.

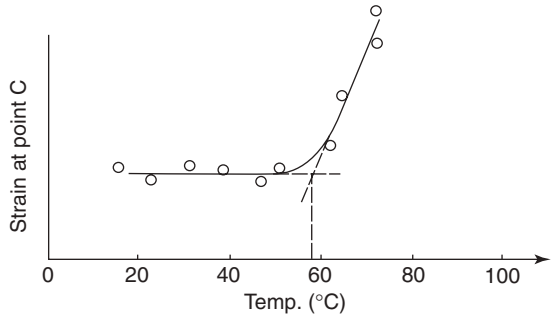

4.31 Change in strain at end of yield region in wet wool (point C in Fig. 4.4). [*From Chapman.*[15]]

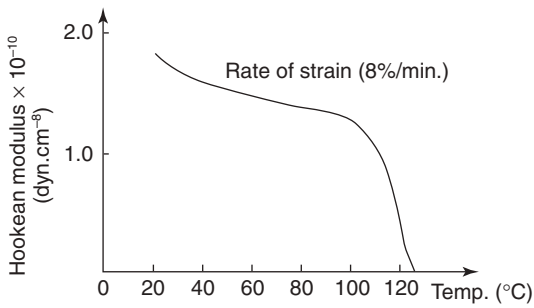

4.32 Change in initial modulus of wet wool with temperature. [*From Chapman.*[15]]

In wet wool, the X-ray diffraction pattern of α-keratin is lost at about 130 °C, indicating a melting of the intermediate filaments (IFs). In dry fibres, a melting endotherm occurs at around 225 °C.

4.3.7 Ageing and setting

The stress relaxation of wool has been referred to in Section 4.3.3. However, it can be viewed in another context as 'ageing' of the fibre. This is particularly important in relation to wrinkling and wrinkle recovery in wool fabrics. In effect, the ageing of bent fibres in the fabric, due to stress relaxation, means that they have been 'set' in a new form with changed properties.

Setting can be accomplished more rapidly by other treatments. Feughelman[36] studied the behaviour after setting in boiling water for 1 hour. Figure 4.34 shows the stress–strain curves in water at 20 °C for the original unset fibre and a fibre that had been set at 10% extension. Both because of the increased set length and a reduction in the initial modulus, the start of the

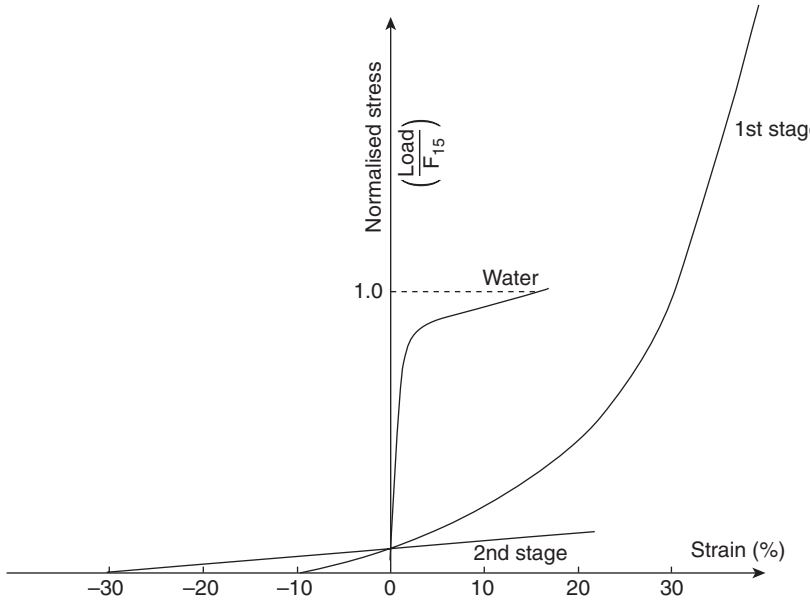

4.33 Stress–strain curves in water and in LiBr solution after first- and second-stage supercontraction. [*From Chapman.*[35]]

yield region at A is shifted to a much higher extension, when based on the original length. The yield slope is unchanged and the end of the yield region at B is shifted only slightly to a higher extension. Feughelman found that the change was only partial after setting for just one minute. The points A and B were in the same positions as in Fig. 4.34, but the fibre was not set: its length under zero stress was unchanged. The initial part of the curve started from 0% extension and followed a sigmoidal path, with high-low-high slopes, to the start of the yield region at A. Feughelman also found that releasing the fibre, after 1 hour set, in water at 100 °C for 1 hour, restored the fibre almost to its original length and stress–strain curve. Release at 120 °C led to supercontraction.

As described in Section 7.13, setting is assisted by chemical treatments that attack disulphide bonds, and may be locked in if more permanent chemical cross-links are formed.

4.3.8 Fibre friction

Wool has the unusual feature of a directional frictional effect (DFE). It is harder to pull against the scales than with them. For wool on wool, there are three options: (1,2) fibres with roots and tips opposed, pulled with or against the scales; (3) fibres with roots and tips at same end, pulled either

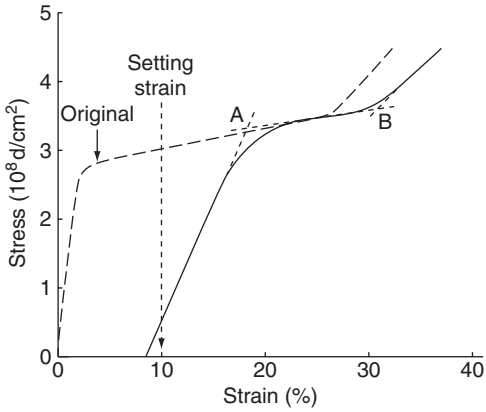

4.34 Stress–strain curves, unset and set at 10% extension in boiling water. [*From Hearle et al.*[37]*, based on measurements by Feughelman.*]

way. For wool on another substrate, there are the two options of with or against the scales. Typical experimental results are given in Table 4.4. As with all fibres, the values of the coefficient of friction μ depend on the state of the surfaces, particularly the presence of lubricants, and the environmental conditions. It is also found that Amontons' Law is not strictly followed, so that μ is not a constant independent of normal load, but is merely a ratio of friction force to normal load.

4.4 Structural mechanics

4.4.1 The chemical background

As is clear from other chapters in this book, wool is composed of a complicated cocktail of proteins and other chemical substances. This means that the thermal and mechanical responses of the fibres are determined by a variety of interatomic and intermolecular bonds and a diversity of structural forms. The mechanics of most of the properties is understood qualitatively, and there are some quantitative theories. Much detail remains to be worked out, but this should be achieved through advances in computer modelling and in analytical techniques, which define structure more precisely. The different parts of wool fibres that influence mechanical properties are shown in Fig. 4.1.

The keratin proteins in the intermediate filaments (IFs) can, to a first approximation, be regarded as forming microfibrillar crystals with α-helical chains intra-molecularly linked by hydrogen bonds, though an idealised behaviour will be modified by the presence of various side-groups. Under

Table 4.4 Friction of wool [From: Morton and Hearle[5]]

	with scales	against scales	same direction
Wool on wool – static	0.13	0.61	0.21
– kinetic	0.11	0.38	0.15
Wool on rayon – static	0.11	0.39	
– kinetic	0.09	0.35	
Wool on nylon – static	0.26	0.43	
– kinetic	0.21	0.35	
Wool on wool – crossed fibres	0.20–0.25	0.38–0.49	
Pair of twisted wool fibres – dry	0.11	0.14	
– wet	0.15	0.32	
Unswollen wool, swollen** ebonite	0.58	0.79	
Swollen* wool, unswollen ebonite	0.62	0.72	
Swollen* wool, swollen** ebonite	0.65	0.88	
Wool on ebonite – polished surface	0.60	0.62	
– rough surface	0.50	0.61	
Wool on horn: dry	0.3	0.5	
Wool on horn: wet, pH 4.0			
– untreated	0.3	0.6	
– chlorine treated	0.1	0.1	
– alcoholic KOH treated	0.4	0.6	
– sulphuryl chloride treated	0.6	0.7	

* in water ** in benzene.

tension, a crystal lattice transition is observed, extended-chain β-crystals form and the hydrogen bonds become inter-molecular. Terminal domains (tails) of the keratin molecules contain cystine and project into the matrix. The keratin-associated proteins of the matrix are more complicated. The mechanical role of the glycine-tyrosine-rich proteins is not understood, but the cystine-rich proteins constitute a cross-linked network, within the globular molecules, between globules and connecting to the terminal domains of the IF proteins. In the dry state there will be hydrogen bonding between matrix protein segments, but, in wet fibres, absorbed water will give a mobile structure. Other intermolecular bonds will also influence the mechanical response.

The cell membrane complex has a different chemistry. The link to mechanics has been little investigated, but the presence of lipids means that it is probably a fairly weak material. The mechanical responses of the various layers of the cuticle also need more study.

4.4.2 The fibril–matrix composite

The main features of the stress–strain relations can be explained in terms of an axially oriented, parallel assembly of fibrils (IFs) in an amorphous matrix. Feughelman[38] laid the foundations of the theory with the two-phase model shown in Fig. 4.35. Swelling of the matrix by absorbed water, which pushed the fibrils apart, explained the high transverse swelling and low axial swelling of wool. The initial extension in the Hookean region is resisted mainly by the deformation energy of the hydrogen-bonded α-helices in the fibrils, with a small contribution from the matrix. Lower shear and transverse moduli are determined mainly by the softer matrix.

Quantitative analysis of the anisotropic mechanical properties would follow composite theory. For elements in parallel, which applies to the axial extension of the two-phase model, the mixture law adds forces or averages moduli. For elements in series, extensions are added or compliances averaged. Across circular units in a matrix, as applies to the shear and transverse response of the two-phase model, the stress distribution is more complicated, but the predictions tend to be closer to the series model. A three-dimensional finite-element analysis of the anisotropic elasticity was carried out by Curiskis[39,40], but the detailed predictions have been criticised by Postle *et al.*[26 page 23]. The possible role of breakdown of the cell membrane complex or elsewhere, which would give the observed yielding under transverse stress, is discussed in Section 4.4.4.

The two-phase model was extended to cover the large-strain extension and recovery behaviour by Chapman.[41]* The model results from a proper analysis of the mechanics of the composite system of fibrils and matrix, both of which have specific load–extension properties.

For the fibrils, a plot of free energy against extension will have the form shown in Fig. 4.36(a), which is based on a diagram by Feughelman.[9] The energy minima at A and B correspond to the coiled and extended crystal forms. Differentiation gives the force–extension curve shown in Fig. 4.36(b). OA is the extension of the α-helices and FC of the β-crystals. For infinitely large crystals, the extension would jump from A to C, because of the instability of a decreasing force region. At intermediate extensions, both forms

*There was an earlier theory by Feughelman and Haly[42], based on an alternation of X-zones, which extended in the yield region, and Y-zones, which extended in the post-yield region. There were subsequent detailed variations of this model, and in 1994 Wortmann and Zahn[43] suggested an explanation in terms of the IF structure. In the same year, Feughelman[44] suggested another model, which was based on separate globular molecules surrounded by water in the matrix. A review by Hearle[28] concludes that the Chapman model and its later developments, as described here, are basically correct, though enhancements are needed to take account of more complicated structural details.

would be present along DF at the force for equilibrium between α and β, which is given by the slope of the line AB in Fig. 4.36(a). In small crystals, thermal vibrations will cause the jump to occur at the lower force H in Fig. 4.36(b). The expected force–extension relation for the fibrils is thus OHJFC. Along JF, the fraction of α will be decreasing and of β increasing. For the ideal α-helix, the extension to F is 120%, but, for the actual IFs, it is probably only 80%, as some parts are not able to change to the β-crystalline form. In practice, wool fibres will break at around 50% extension, marked by the point G.

On the Chapman model, the matrix in the wet state is assumed to act as a rather highly cross-linked, swollen rubber. The matrix stress–strain curve can be derived from the supercontraction experiments shown in Fig. 4.33. Following the X-ray diffraction evidence, it is assumed that the α-crystals are disrupted in first-stage supercontraction, so that the stress–strain curve

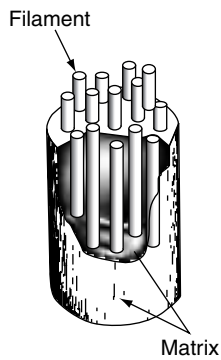

4.35 Feughelman's[38] two-phase microfibril–matrix model. [*As drawn in Postle et al.*[26]]

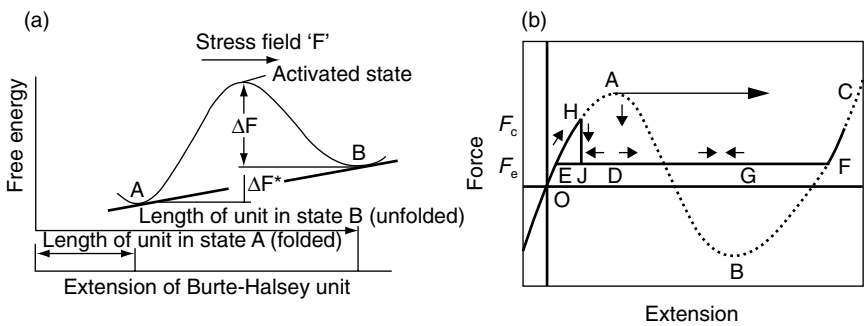

4.36 (a) Free-energy diagram for α → β transition. (b) Force diagram. [*From Hearle.*[28]]

is then dominated by the matrix. If the matrix ceases to contribute after second-stage supercontraction, the small resistance to extension is the residual effect of the disrupted IFs. Subtraction of the stress–strain curve after the second stage from that after the first stage thus gives a prediction of the matrix stress–strain curve, as shown in Fig. 4.37(a). In Fig. 4.37(b), it is shown that this curve is close to a theoretical rubber elasticity curve, based on the inverse Langevin function form, with two free links between junction points. The deviation at high stress can be attributed to some rupture of cross-links, which leads to the observed loss of some recovery from extensions over 30%. The maximum extension of the rubber-elasticity curve is about 50%, and this defines the limit at which the matrix will rupture and wool fibres will break. Higher extensions can be achieved, as was done by Bendit[45], if cystine cross-links are allowed to break by treatment in hot water. This leads to the maximum extension of 80% for completion of the $\alpha \rightarrow \beta$ transition.

In the Chapman model, the composite fine structure is treated as a fibril, with helical chains, in parallel with an amorphous matrix, with the two linked at intervals to give a series of zones, as shown in Fig. 4.38. Originally, this form was chosen for simplicity in modelling, but now the links correspond to the IF keratin tails, which are cross-linked to the KAPs in the matrix. The stress–strain curves of the two components of the wet fibre are shown in Fig. 4.39(a), based on the above arguments. Up to 2% extension, Fig. 4.38(a), both components extend together, but, as described above, almost all the stress comes from the fibrils. When the critical stress is reached, one of the zones, arbitrarily selected either due to variability or thermal vibration, opens from the α helix to the β extended chain. The tension in the fibril drops to the lower equilibrium value and the matrix extends to make up the tension. There would be an infinitesimal drop in tension, but this is picked up by further extension, so that further zones continue to open. The stress through the yield region, Fig. 4.38(b), remains constant and equal to the IF critical stress plus the small contribution of the matrix at 2% extension. At 30% extension, Fig. 4.38(c), all zones have opened. Further extension in the post-yield region, Fig. 4.38(d), causes the matrix stress to increase. In recovery, Fig. 4.38(e), there is no critical factor and the zones all contract together until they disappear and the initial stress–strain curve is rejoined. With the values shown in Table 4.5, the predicted stress–strain curve is shown in Fig. 4.39(b). This is identical with the experimental stress–strain and recovery curves, if the variability that causes the slope in the yield region is absent.

At humidities below 100%, intermolecular hydrogen bonds stiffen the matrix. This gives a larger matrix contribution to the stress and thus increases the initial slope and the yield stress. In the initial and post-yield regions, the matrix stress can be calculated by subtracting the assumed fibril

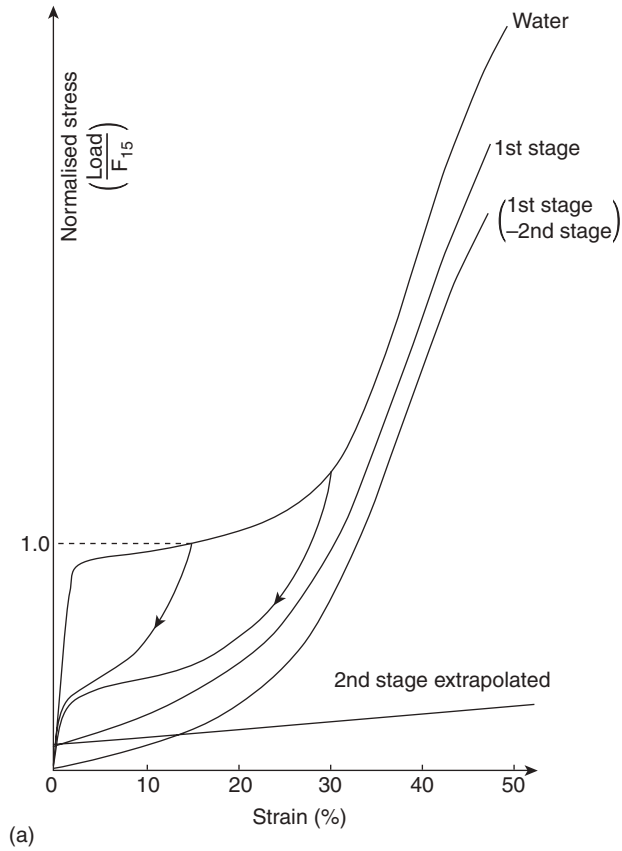

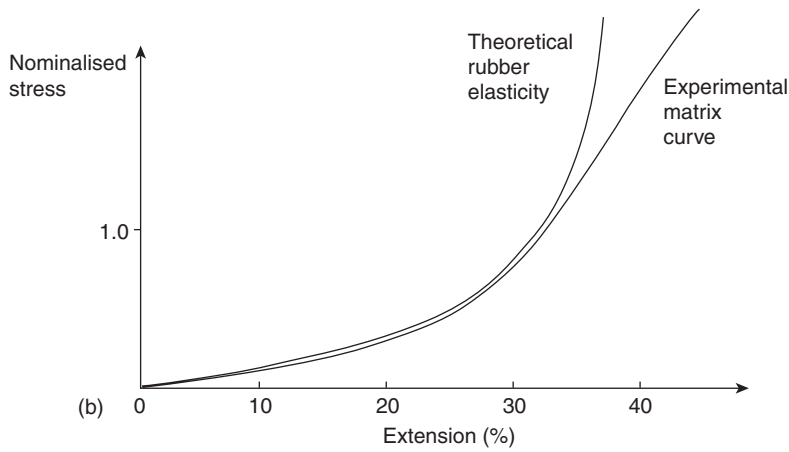

4.37 (a) Stress–strain curves of wool after first- and second-stage supercontraction, and for (first stage – second stage), which is assumed to be the matrix curve. The curve for wool in water, which in recovery is almost parallel to the matrix curve, is shown for comparison. (b) Comparison with theoretical rubber-elasticity curve. [*From Chapman.*[35]]

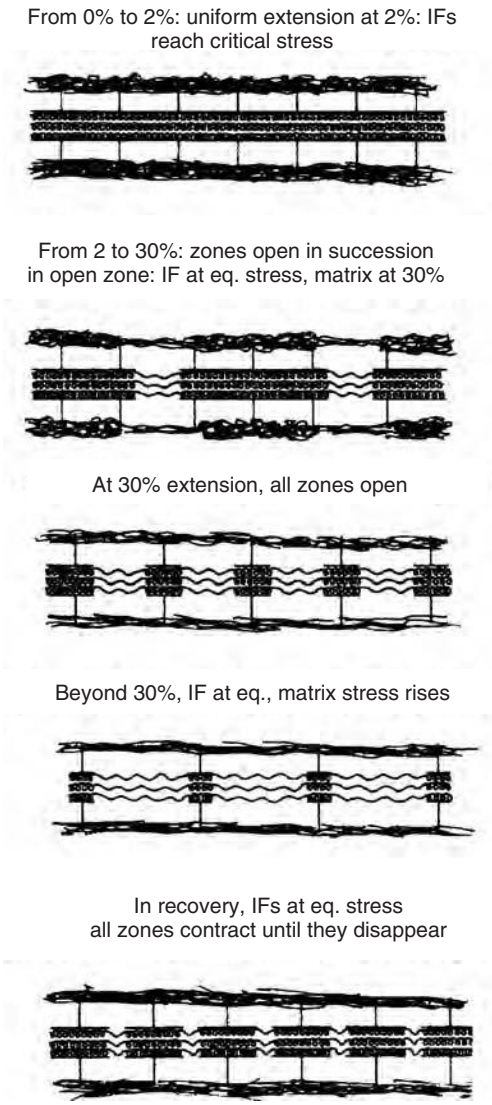

4.38 Schematic representation of the sequence of changes in the Chapman model. [*From Hearle.*[28]]

stress from the experimental curves shown in Fig. 4.6. For the intermediate extensions, calculation is not possible, but Fig. 4.40 shows matrix stress–strain curves interpolated in this region.[37] They are typical of an amorphous polymer with hydrogen bonds that are broken at a yield stress.

Setting can be explained[37] on the assumption that the rupture and reformation of cross-links relieves the stress and shifts the origin of the matrix

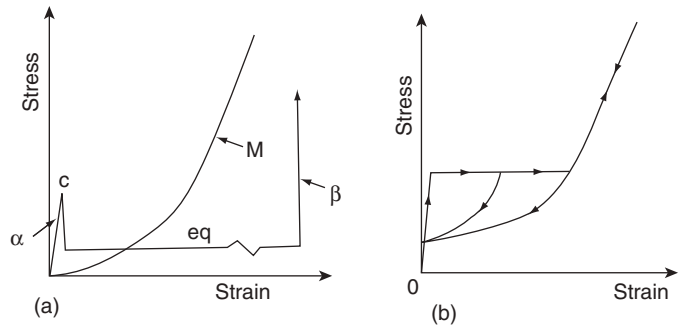

4.39 (a) Stress–strain curves for fibril and matrix; (b) Predicted stress–strain curve of composite. [*From Hearle.*[28]]

Table 4.5 Controlling parameters for Chapman model [From: Hearle[28]]

Parameter	Value	Determines	Notes
Microfibrils			
α modulus	1.75 GPa	Initial fibre modulus (plus small matrix contribution)	Similar to theoretical calculation
Critical stress α → β trans'n	0.035 GPa	Fibre yield stress (plus small matrix contribution)	Reasonable at 2% strain
Equil'm stress α → β trans'n	0.07 GPa	Junction of extension and recovery curves	Reasonable on basis of Fig. 4.36
β modulus	1.75 GPa	Additional microfibril extension in post-yield region	Actually higher; negligible effect
α → β strain	80%	Extension in opened zones	From X-ray diffr'n expt's; less than ideal α-helix
Matrix			
# Nonlinear stress/strain	See Fig. 4.37(b)	Post-yield and recovery curves (plus microfibril contribution)	From supercontr'n expt's & rubber elasticity theory
In'l modulus	0.35 GPa	Addition to microfibril tension	Follows from #
Extension at critical stress	30%	End of yield region	Follows from #
Ideal max'm extension	40%	Limiting extension if no cross-link failure	Follows from #
Actual max'm extension	50%	Fibre break extension and strength	Greater than ideal max'm due to cystine bond break

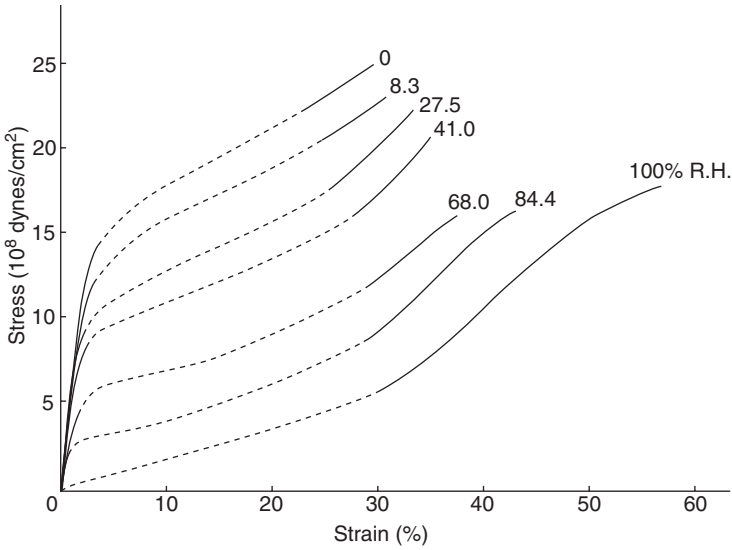

4.40 Predicted matrix stress–strain curves at different humidities. Dotted lines are interpolated between calculated curves from model. [*From Hearle et al.*[37]]

stress–strain curve to the setting strain, as shown in Fig. 4.41(a). Application of a sequence similar to that shown in Fig. 4.34 gives the new stress–strain curve, shown in Fig. 4.41(b). The positions of the points A and B are found to be the same as in the experimental curves of Fig. 4.34, but something different happens in the low-stress region.

Visco-elasticity in dry wool in the Hookean region is explained by the progressive breakage of hydrogen bonds in the matrix due to thermal vibrations. This will be intensified at larger strains. If the thermal and chemical conditions are right, other bonds, such as cystine cross-links, will also show time-dependent breakage. The lowering of the critical condition for the $\alpha \rightarrow \beta$ transition due to thermal vibrations, as shown in Fig. 4.36(a), is another source of time-dependence. Detailed theoretical treatments of these effects follow the classical visco-elastic models, either in their mathematical formulations[26] or by adding viscous elements to the computation of the two-phase model.[46] By adjusting parameters, it is possible to fit experimental results, but more detailed understanding and modelling is needed in order to derive predictions from first principles.

4.4.3 The ortho-cortex and fibre crimp

The two-phase model with fibrils parallel to the axis of the fibre, as shown in Fig. 4.35, and the subsequent treament of the fibre mechanics, applies

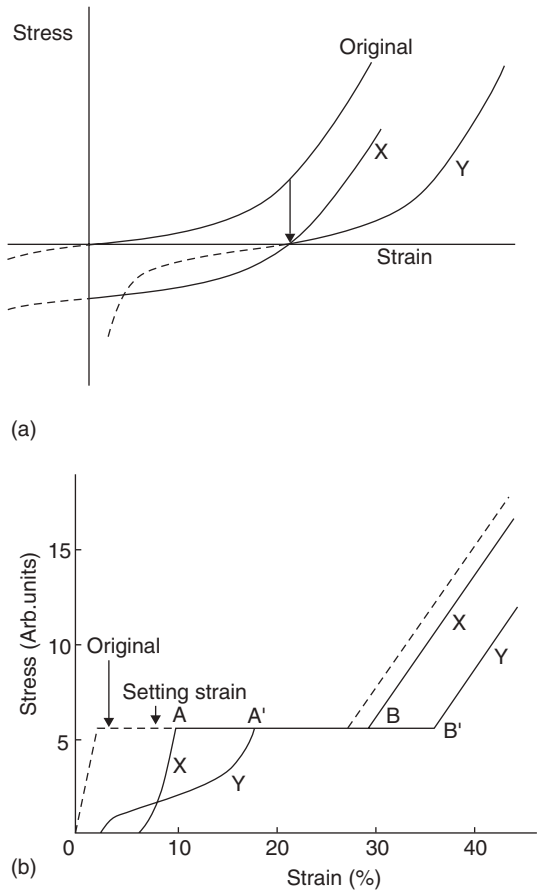

4.41 (a) Postulated changes in matrix stress–strain curve after setting. (b) Calculated behaviour of set fibres. [*From Hearle et al.*[37]]
Note: The X lines, which do not give a reasonable prediction, follow a vertical shift of the stress–strain curve; the Y lines with a horizontal shift give a prediction similar to the experimental results.

strictly only to the para-cortex of wool and, with some detailed modification of input parameters, to the meso-cortex. In the ortho-cortex of wool, the IFs (microfibrils) are bundled together in macrofibrils. Electron microscope pictures show circular IF cross-sections at the centres of macrofibrils, becoming increasingly elliptical towards the circumference. This implies that the IFs and the associated matrix follow helical paths in the macrofibrils. Electron microscope tomography[47] enables quantitative measurements of twist angles to be made. The structure is like that of a twisted yarn. Similar theory will apply, though account must be taken of the shear stress between IFs and this will lead to a change in tensile properties, which can

be approximated as a reduction of stress at a given extension by the factor $\cos^2\alpha$, where α is the twist angle at the surface of a macrofibril.

A more important consequence is the influence of dimensional changes associated with moisture content, as analysed by Munro and Carnaby.[48] The simplest assumption is that the wool fibre is straight when wet, since this is the state in which it is formed. The IFs are then widely separated by the swollen matrix. Drying the fibre will cause a lateral contraction that will reduce the twist angle and cause the macrofibril to extend. The increased stress-free length of an isolated macrofibril would depend on a balance of contraction at the circumference and extension at the centre. However, on the other side of the wool fibre, the lateral contraction of the para-cortex will not cause any extension, because the IFs are parallel to the fibre axis. Consequently, the fibre acts like a bimetallic strip and bends to minimise the deformation energy. The longer orthocortex will take the outside of the bend and the shorter paracortex the inside, as is observed experimentally.[49,50] This is the source of crimp in wool fibres.

There is some uncertainty about the detail of the helical form. If the ortho–para boundary rotates along the fibre, it would automatically generate a helix. However, if the boundary remains in the same transverse direction, the minimum energy state would be a tight coil, but, to form this from the straight fibre, it is necessary for the fibre to twist. If twisting is allowed, the intermediate state at a given fibre length would be a unidirectional helix; if it is not, alternating right- and left-handed helices would form, as in bicomponent synthetic fibres.

4.4.4 Fibre strength and the cell membrane complex

On the Chapman model, as described in Section 4.4.2, the matrix would break at a lower extension than the IFs, and would trigger fibre breakage at around 50% extension. However, the wool fibre is a composite at a number of levels, and it is likely that the system of cells bonded together by the cell membrane complex (CMC) plays a part in determining the form of breakage. Once a crack started in the matrix of one cell, it would be expected to propagate across the cell. The CMC will act as a weak bond, which, as in fibre composites, blocks crack propagation. However, there will be stress transfer from the ruptured cell to neighbouring cells, which causes them to break in a nearby region. This gives rise to the granular breaks shown in Fig. 4.26.

The above argument applies to the intrinsic strength, which gives the upper bound in Fig. 4.25. There are many possible causes of lower values of strength. As already mentioned, if the fibre is variable, failure at the weakest link will give a lower apparent strength when related to the average

fibre thickness. Lower intrinsic strength will result from any damage or defects in the fibres.

Weakness in the CMC is another, more fundamental, possibility.[51] For short fibre composites, the strength is reduced, compared to a system without slip, by a slippage factor *SF*, which is given by equation [4.3]:

$$SF = 1 - (1/4)(S/B)(D/L) \quad [4.3]$$

where *S* is the tensile strength of the cell, acting as a short fibre in the composite, *B* is the bond strength of the CMC between cells, *D* is the cell diameter and *L* is the cell length.

In 'good wool', with *B* reasonably high and (*D*/*L*) small, *SF* should be close to 1, but, if there are thick, short cells with weak CMC, then there will be appreciable loss of strength.

The slippage effect will be greater in the transverse direction when (*D*/*L*) is equal to one. This is the most likely cause of the yielding in transverse extension of porcupine quill, as found by Feughelman and Druhalla.[27]

Breakdown of the CMC will lead to the multiple split ends that are often seen in failure of wool in fatigue situations. The transverse axial cracks are a natural consequence of the buckling of aligned elements within the structure.[52]

4.4.5 Fibre friction and the scales

Qualitatively, the scales on the wool fibre would be expected to give a ratchet-like action, due to scales interlocking with one another or catching on asperities on a surface. This would give rise to the directional frictional effect. Figure 4.42 shows the various possible interactions, and from the geometry it is intuitively obvious that motions against scales, Fig. 4.42(b,d), will give more resistance than with scales, Fig. 4.42(c,e). For fibres in the same direction, Fig. 4.42(a), the friction will have an intermediate value.

Lincoln[53] has given a more detailed analysis based on the components of normal load and frictional force, as shown in Fig. 4.43(a). If *F* is the frictional force and *N* is the normal load, Amontons' Law, $F = \mu N$, has a constant coefficent of friction μ. Polymeric fibres are generally found to follow a power law: $F = aN^n$. This formulation implicitly assumes that the normal load and frictional force are respectively perpendicular and parallel to the surfaces, both locally and generally. For the scales on wool, this is not so. In Fig. 4.43(a), *W* and *F* are the components related to the overall surface, *N* and *P* are the components related to the local plane of contact, which makes an angle θ with the overall surface plane. Putting $P = aN^n$, the forces are related by equation [4.4].

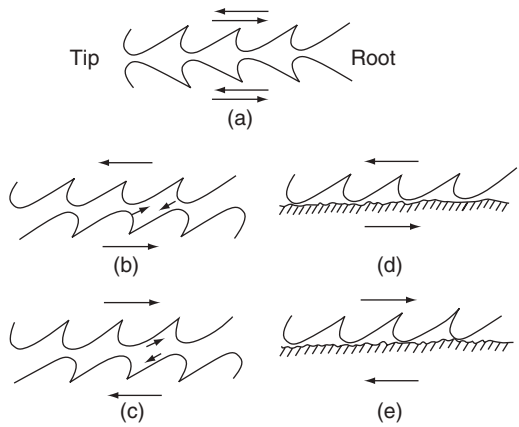

4.42 Directional friction in wool: (a) between fibres lying in same direction; (b) between fibres against scales; (c) between fibres with scales; (d) on plane surface against scales; (e) on plane surface with scales. [*From Morton and Hearle.*[5]]

$$F\cos\theta - W\sin\theta = a(W\cos\theta + F\sin\theta)^n \qquad [4.4]$$

The frictional force increases rapidly as θ goes from negative values, i.e. moving away from the slope, to positive values, as in Fig. 4.43(a). Contact with a wool fibre as shown in Fig. 4.43(b) will have different angles, depending on which part of the scale is in contact. These may be simplified as a saw-tooth with two angles, α and β. Combining positive and negative values of α and β, as appropriate, leads to the frictional forces shown in Fig. 4.43(c), in which the mean force against the scales is higher than the mean force with the scales.

4.5 Electrical properties

4.5.1 Dielectric constant and loss factor

At the base level for dry wool, the dielectric constant of wool is about 1.5, and this will result from dipolar groups in the protein and other molecules. In practice, the major influence is that of water. H_2O is a permanent dipole, and its orientation in an electric field determines the dielectric constant ε. The lag in responding to an alternating field determines the loss factor $\tan\delta$. The structural features that influence these values are the amount of absorbed water and the firmness with which it is bound; the test conditions that change the values are frequency and temperature.

A measurement problem is that the only easy way to measure dielectric properties is on a fibre assembly. Hearle[7,54] made tests on yarns wound

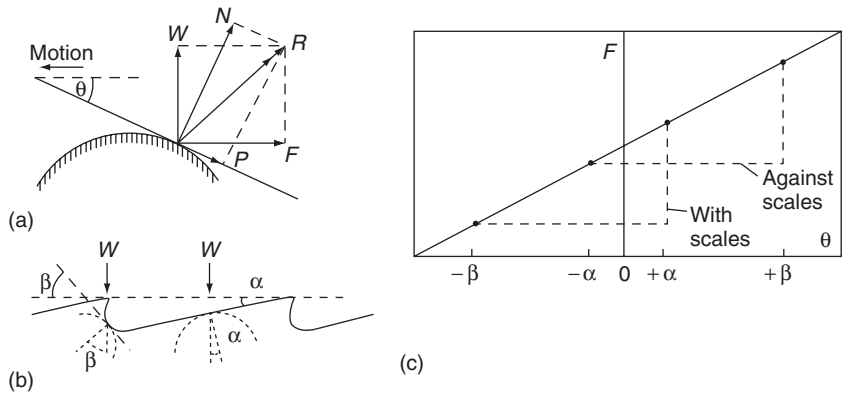

4.43 (a) Frictional contact at an angle to the overall surface. (b) Different angles of contact on wool scales. (c) Combined effect with and against scales. [*From Morton and Hearle.*[5]]

between two cones. The results are shown in Fig. 4.44. The dielectric constant and power factor rise steeply at higher moisture contents and lower frequencies.

4.5.2 Electrical resistance

Electrical current in wool is carried either by charged ions present as impurities or by the mobility of protons in hydrogen bonds. According to a theory by Hearle[55], only dissociated ions are free to move, and the degree of dissociation depends on the dielectric constant ε through its influence on the dissociation energy of two charged particles. Application of the Law of Mass Action leads to equation [4.5]:

$$\log R = (A/\varepsilon) + B \qquad [4.5]$$

where R is the electrical resistivity and A and B are constants.

Changes in ε cause orders-of-magnitude changes in resistance, because of the logarithmic dependence. Empirically, it was found that at higher values of moisture content M, $\log R$ varied linearly with $\log M$. Figure 4.45 shows the variation of resistance with moisture content and compares the theoretical and experimental results. Up to about 6% moisture content, the resistivity of wool is constant with a value over 10^{12} ohm cm or, in mass terms, 10^{12} ohm g/cm^2. The drop in resistance starts at a higher moisture content than in cotton and this reflects the way in which the first absorbed water is firmly bound. A comparison against relative humidity is shown in Fig. 4.46. Wool lies between the more conductive cellulose fibres and the less conductive synthetic fibres.

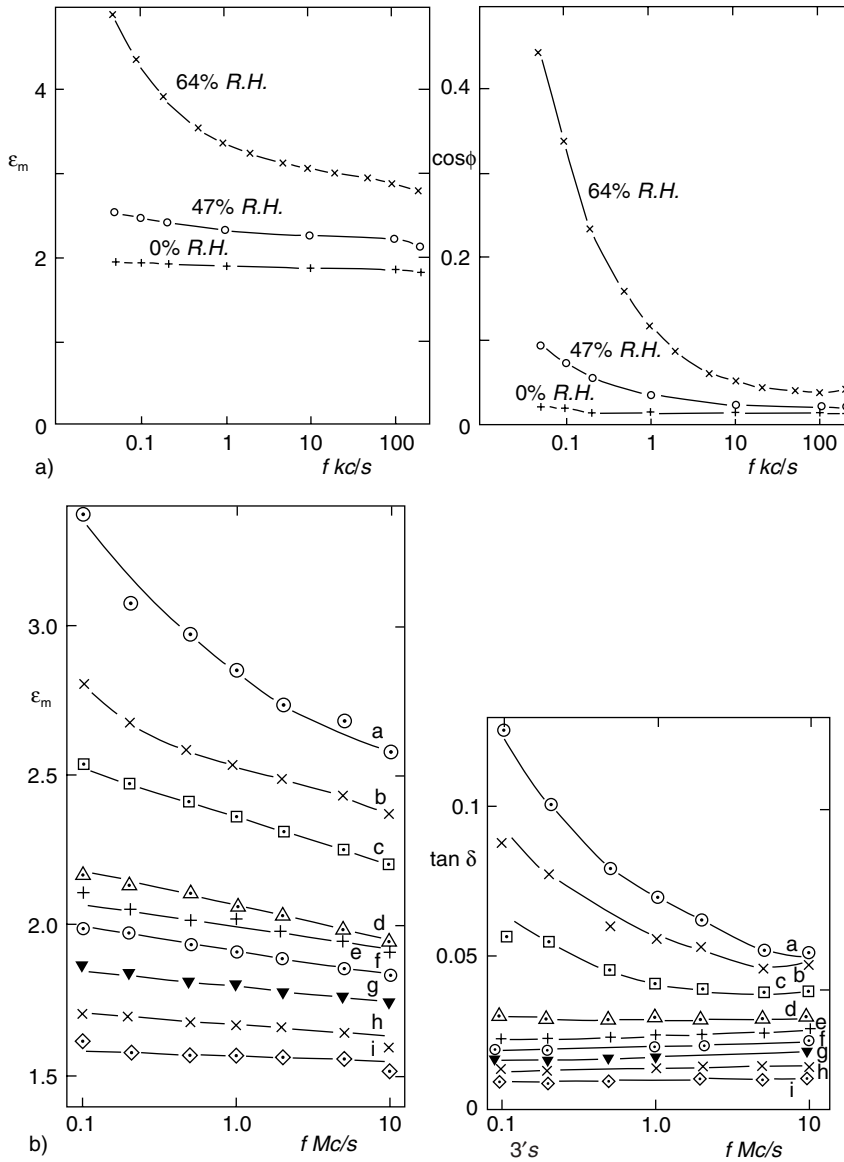

4.44 Dielectric constant and loss factor of wool yarns with a packing factor of 52–53%. (a) By bridge method at lower frequencies[7] (the loss is expressed by the power factor $\cos\phi$, which equals $\sin\delta$); (b) By a resonance method at higher frequencies.[54]

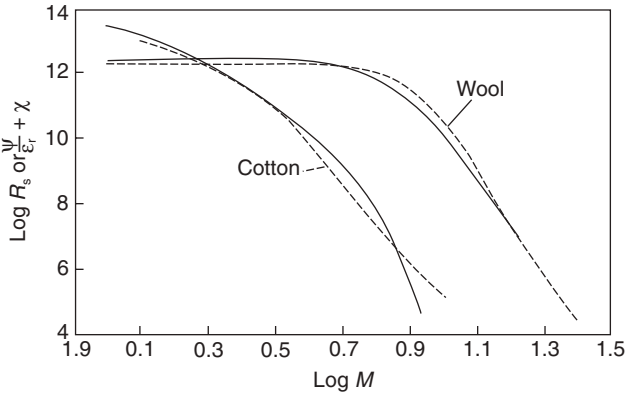

4.45 Log–log plot of resistance against moisture content, showing a comparison of experimental values (full lines) and theoretical predictions from equation [4.5] (dotted lines). [*From Morton and Hearle.*[5]]

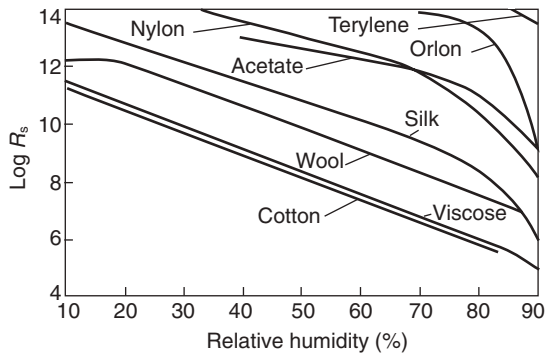

4.46 Plot of resistance on a logarithmic scale against relative humidity for a variety of fibres. [*From Morton and Hearle.*[5]]

4.5.3 Static electrification

Static electricity is easily generated when two different surfaces are separated. Typically this occurs in rubbing or in walking on wool carpets. A determining factor in the detection of static charging is how fast the charge can leak away. If the material is a perfect insulator, the limiting charge is given by conduction across the gap between the surfaces as they separate but, if the material is a moderate conductor, conduction can occur back through the material to the unseparated region. If the material is a good conductor, all the charge can flow back and none is left on the material. For practical time scales, static charges begin to drop from the maximum

limiting value when the resistivity falls to 10^{10} ohm cm, and will be very small below 10^{6} ohm cm. The values in Fig. 4.46 show that wool will suffer from appreciable static charging below 60 to 70% RH. Static electrification is described in detail by Morton and Hearle.[5]

4.6 Yarns and fabrics

4.6.1 Structural mechanics of fibre assemblies

In general terms, the mechanics of wool yarns and fabrics follows treatments that are common to all textiles. These are described in books.[56,57] An account that is specifically related to wool is given by Postle *et al.*[26] Hearle[58] includes nonwovens. The extensive work on fabric hand and the KES-F testing system, which is particularly relevant to the effects of finishing of wool fabrics, has been reviewed by Kawabata and Niwa.[59]

In addition to the particular tensile and other properties, the special features of wool are fibre crimp, which leads to high bulk and softness, and scales, which lead to felting. Good recovery properties are also beneficial, and especially the regeneration of properties by washing. Setting, whether temporary by drying or permanent by chemical cross-linking, maintains the form of yarns, fabrics and garments.

4.6.2 Wool yarns

Most wool yarns are twisted structures. Twist, or the alternative of entanglement by felting, is necessary to hold staple fibres together. The effect of obliquity is to reduce the stress at a given extension, but wrapping round in a curved path generates transverse pressure and hence axial friction, which grips the fibres. An approximate analysis[56] gives the effect on the yarn stress–strain curve in terms of the surface twist angle α and a factor k that depends on the resistance to slip:

$$\begin{aligned}&\text{(yarn stress at given extension/fibre stress at same extension)}\\&\quad = \cos^2\alpha(1 - k\ \text{cosec}\ \alpha)\end{aligned} \qquad [4.6]$$

The first term is the direct effect of obliquity. The second term is the reduction in stress due to slip from fibre ends. The factor k is proportional to $(a\ Q/\mu L^2)^{1/2}$. This shows the more effective gripping of fibres with small radius a, large length L, and high coefficient of friction μ, in yarns with a short migration period Q and high twist α. The twist is given in operational terms by:

$$\tan\alpha = 0.0112(1/\varphi\rho)C^{1/2}T \qquad [4.7]$$

where φ is the packing factor, ρ is fibre density in g/cm^3, C is yarn linear density in tex, and T is twist in turns/cm.

As $(1 - k\,\mathrm{cosec}\,\alpha)$ decreases from a limiting value when $k\,\mathrm{cosec}\,\alpha << 1$, the central length of fully gripped fibre becomes smaller. Equation [4.6] breaks down below $(1 - k\,\mathrm{cosec}\,\alpha)$ equal to $^1/_2$. The fibres are no longer fully gripped anywhere and there is cumulative slippage. This is the turnover condition between self-locking yarns and draftable rovings.

Figure 4.47(a) gives examples of the stress–strain curves for worsted and woollen rovings twisted on a laboratory twister[60], and Fig. 4.47(b) gives a comparison of the experimental values of modulus and strength with values predicted from equation [4.6] with fitted values of *k*. The more irregular woollen structure does not fit the theory and is much weaker than the worsted structure. Modulus results for the worsted yarn can be fitted to equation [4.6], but the strength values require an additional numerical factor, which reflects a higher effective fibre strength in yarns than in fibre tests.

A more detailed theory for wool yarns in which there is negligible slip from fibre ends is given in Postle *et al.*[26] This takes account of the bulkiness of wool yarns, and the reduction in volume during extension as the outer fibres compress the underlying structure. The shortest path hypothesis provides a useful procedure. Because fibres are slender, the energy needed to bend and twist them is small and can be neglected, so that they take up the shortest available path. Once a fibre has been pulled into such a path, any further yarn extension requires fibre extension, which is much more strongly resisted and dominates the deformation energy. Following the early work of Carnaby and Grosberg,[61–63] a number of more detailed analyses have been made using more elaborate mathematical and computational techniques. However, the underlying difficulty is to have an adequate description of the complex fibre arrangement in wool yarns, which can have a major influence on when the structure jams so that fibres are forced into extension. The more difficult problem of the formation of yarn structure needs to be solved as a prelude to analysing the mechanics of the structure.

4.6.3 Fabric mechanics

Postle *et al.*[26] provide a full account of work on the mechanics of woven and knitted fabrics. In general, deformation under low forces depends on the resistance to bending and twisting of yarns, so that the initial modulus is low. When tensions are high enough to straighten yarns or jam the fabric, the forces increase and follow the resistance to yarn extension. Because fabrics are thin, they have a low bending resistance. However, the double curvature needed for good drape and handle also requires in-plane deformation.[64] This is found in woven fabrics by a trellis action, which gives very low resistance to shear, and in knitted fabrics by the loop structure, which gives a low resistance in all directions.

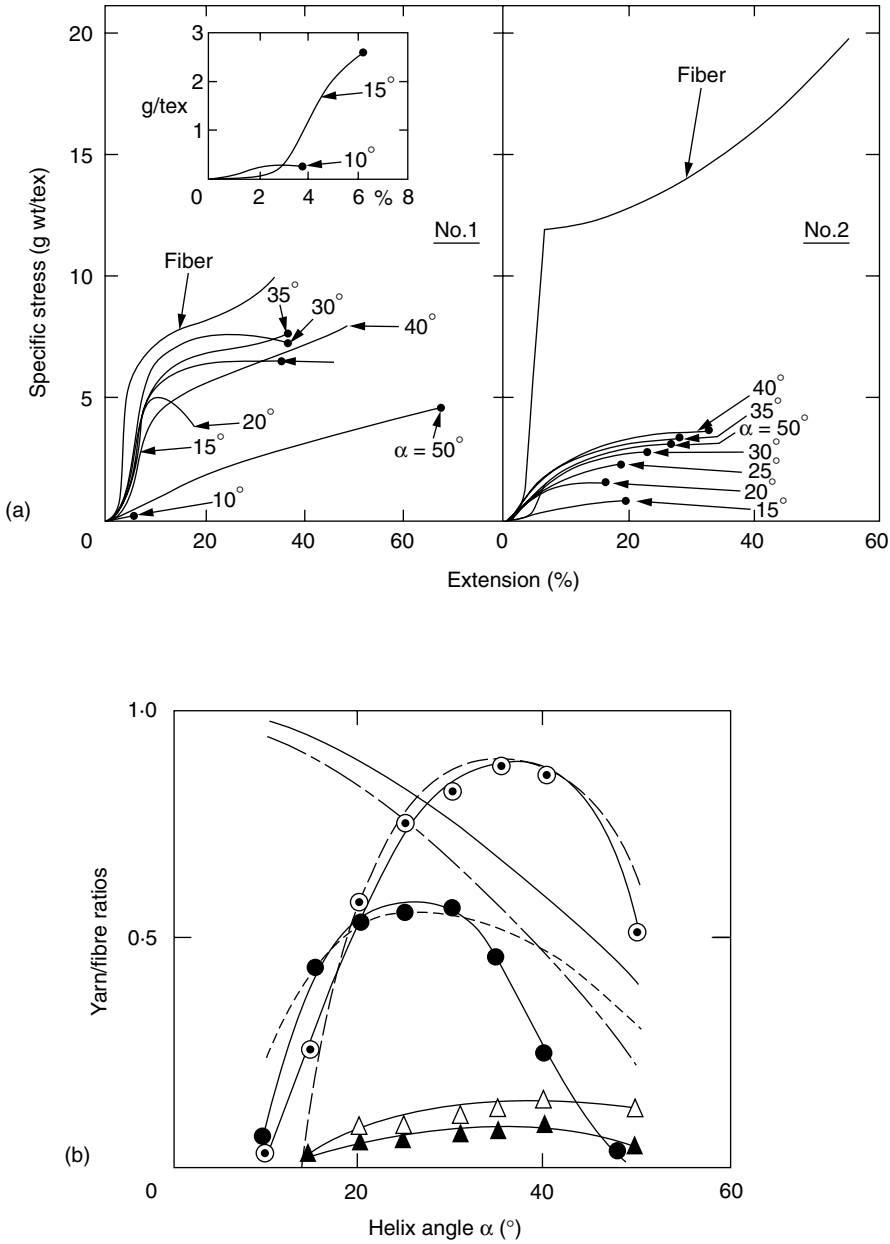

4.47 a) Stress–strain curves of fibres and twisted rovings. No. 1 – worsted. No. 2 – woollen. (b) Comparison of theory and experiment. No. 1 – worsted. Yarn modulus: black circles, experimental; short dash line, theoretical plot of $\cos^2\alpha(1 - 0.133\,\mathrm{cosec}\,\alpha)$. Yarn strength: open circles, experimental; long dash line, theoretical plot of $2.3\cos^2\alpha(1 - 0.24\,\mathrm{cosec}\,\alpha)$. No. 2 – woollen. Yarn modulus: black triangles, experimental. Yarn strength: open triangles, experimental. The two lines coming down from top left are for two theories of effect of obliquity without slip. [*From Hearle and EL-Sheikh.*[60]]

An aspect of particular importance to wool fabrics is the relaxed state of the fabric. After manufacture or finishing, the fabric will have certain dimensions, but relaxation will change these. For knitted fabrics, Munden[65] defined two relaxed states: dry-relaxed for fabrics allowed to recover from knitting stress for at least 24 hours; wet relaxed after wetting and subsequent conditioning. Wrinkling, creasing and crease recovery in wool fabrics, which involve the bending response of wool fibres, have been modelled by Chapman.[66,67]

Wool is used in needled nonwoven fabrics, in which the fibre arrangement generates the friction to provide fabric strength. The active geometry consists of curved fibre paths in the plane of the fabric passing round the 'pegs' (tufts of fibres) that result from the needling action.[68] Needled fabrics are necessarily rather thick and, if they are to be stable self-locking structures, must be compacted, so they lack low in-plane resistance and therefore are limited in drape capability.

Felts are a long-established form of wool fabric, made possible because of the directional frictional effect in wool (see Section 4.4.5). When a mass of wool fibres is agitated, particularly in hot wet conditions when the fibres are very flexible, each fibre moves in the low-friction direction. The roots move forward followed by the tips – in other words, if the fibre direction is defined as root-to-tip, the fibre as a whole moves progressively backward. Each step involves an increase of interlacing with neighbouring fibres. Eventually a highly interlaced, self-locking felt is produced.

4.6.4 Carpets

Wool is used as a carpet fibre because of its bulk, resilience and durability. Carnaby and Wood[69] have reviewed the physics of carpets. Important aspects are comfort and compression, appearance retention, and wear resistance. The compression behaviour is determined by the bending and bending recovery of fibres within the carpet pile. An aspect of this related to appearance is the problem of shading, which can cause great concern to customers. It has been shown that this is due to patches of fibres lying in different directions. In some cases, the cause is clear. For example, the movement in turning a corner provides shear forces in a particular direction, which causes the fibres to bend over from their initial direction to follow the shear. Neighbouring regions which are not walked on, or are subject to a symmetrical pattern of treads, will have fibres that remain lying in the original direction. In cases where there is no obvious cause, it is presumed that there is some asymmetric action at an early stage of the use of the laydown or use of the carpet, which causes the pile to reverse, and that this is intensified by subsequent treading.

Carpet wear has been modelled in terms of fatigue sites that are more-or-less randomly distributed through the carpet pile. This leads to a progressive loss of fibre material. Wear is much more severe in turning-walk trials than in straight walk. The commonest form of fibre breakage is the development of cracks in severely kinked fibres.[70]

References

1 Preston J M, *Modern Textile Microscopy*, Emmott, London, 1933.
2 Speakman J B, Cooper C A and Stott E, 'Wool: moisture relations', *J. Text. Inst.*, 1936, **27**, T183–96.
3 Preston J M and Nimkar M V, 'Measuring the swelling of fibres in water', *J. Text. Inst.*, 1949, **40**, P674–88.
4 Darling R C and Belding H S, 'Textile yarns: moisture absorption at low temperatures', *Industr. Eng. Chem.*, 1946, **328**, 524–9.
5 Morton W E and Hearle J W S, *Physical Properties of Textile Fibres*, 3rd edition, The Textile Institute, Manchester, 1993.
6 Speakman J B, 'An analysis of the water adsorption isotherm of wool', *Trans. Faraday Soc.*, 1944, **40**, 6–10.
7 Hearle J W S, 'Capacity, dielectric constant and power factor of fibre assemblies', *Text. Res. J.*, 1954, **24**, 307–21.
8 WIRA, *Wool Research* Vol 2: *Physical Properties of Wool Fibres and Fabrics*, Wool Industries Research Association, Leeds, 1955.
9 Feughelman M, *Mechanical Properties and Structure of Alpha-keratin Fibres*, UNSW Press, Sydney, 1997.
10 Bendit E G, 'A quantitative X-ray diffraction study of the alpha-beta transformation in wool keratin', *Text. Res. J.*, 1960, **30**, 547–55.
11 Collins J D and Chaikin M, 'The stress–strain behaviour of dimensionally and structurally non-uniform wool fibres in water', *Text. Res. J.*, 1965, **35**, 777–87.
12 Collins J D and Chaikin M, 'Structural and non-structural effects in the observed stress–strain curve for wet wool fibres', *J. Text. Inst.*, 1968, **59**, 379–400.
13 Speakman J B, 'Intracellular structure of the wool fibre', *J. Text. Inst.*, 1927, **18**, T431–53.
14 Peters L and Woods H J, *Protein Fibres* in Meredith R (editor), *Mechanical properties of textile fibres*, North-Holland, Amsterdam, 1956.
15 Chapman B M, 'A review of the mechanical properties of keratin fibres', *J. Text. Inst.*, 1969, **60**, 181–207.
16 Meredith R, 'Textile fibres: comparison of tensile elasticity', *J. Text. Inst.*, 1945, **36**, T147–64.
17 Beste L F and Hoffman R M, 'Resilience of fibres and fabrics: quantitative study', *Text. Res. J.*, 1950, **20**, 441–53.
18 Feughelman M and Robinson M S, 'Some mechanical properties of wool fibers in the "Hookean" region from zero to 100% relative humidity', *Text. Res. J.*, 1971, **41**, 469–74.
19 Katz S M and Tobolsky A V, 'Wool fibres: relaxation of stress', *Text. Res. J.*, 1950, **20**, 87–94.

20 Feughelman M, 'The creep of wool fibres in water', *J. Text. Inst.*, 1954, **45**, T630–41.
21 Danilatos G and Feughelman M, 'Dynamic mechanical properties of α-keratin fibers during extension', *J. Macromol. Sci. – Phys.*, 1979, **B16**, 581–602.
22 Meredith R, 'Dynamic mechanical properties of textile fibres', *Proc. 5th Int. Congress in Rheology 1968*, University of Tokyo Press, 1969, Vol 1, 43–60.
23 Chapman B M, 'The bending stress–strain properties of single fibres and the effect of temperature and relative humidity', *J. Text. Inst.*, 1973, **64**, 312–27.
24 Bendit E G and Feughelman M, 'Keratin' in *Encyclopaedia of Polymer Science and Technology*, Vol 8, 1–44, Wiley, New York, 1968.
25 Mitchell T W and Feughelman M, 'Torsional properties of single wool fibres. Part I: Torque–twist relationships and torsional relaxation in wet and dry fibres', *Text. Res. J.*, 1960, **30**, 662–7.
26 Postle R, Carnaby G A and de Jong S, *The Mechanics of Wool Structures*, Ellis Horwood, Chichester, 1988.
27 Feughelman M and Druhalla M, 'The lateral mechanical properties of alpha-keratin', *Proc. 5th Int. Wool Text. Res. Conf.*, Aachen, 1975, **2**, 340–9.
28 Hearle J W S, 'A critical review of the structural mechanics of wool and hair fibres', *Int. J. Biological Macromol.*, 2000, **27**, 123–38.
29 Kawabata S and Kawashima Y, 'Measurement of the anisotropy in the elastic modulus of cotton and silk fibres', *Proc. 29th Text. Res. Symp.*, Mount Fuji, 2000, 51–8.
30 Woods J, Orwin D F G and Nelson W G, *Proc. 8th Int. Wool Text. Res. Conf.*, 1990, 557–68.
31 Hearle J W S, Lomas B and Cooke W D, '*Atlas of Fibre Fracture and Damage to Textiles*', 2nd edition, Woodhead Publishing, Cambridge, 1998.
32 Baxter S, 'Textiles: thermal conductivity', *Proc. Phys. Soc.*, 1946, **58**, 105–18.
33 Haly A R and Snaith J W, 'Specific heat studies of various wool–water systems', *Biopolymers*, 1968, **6**, 1355–77.
34 Phillips D G, 'Detecting a glass transition in wool by differential scanning calorimetry', *Text. Res. J.*, 1985, **55**, 171–4.
35 Chapman B M, 'Observations on the mechanical behaviour of Lincoln-wool fibres supercontracted in lithium bromide solution', *J. Text. Inst.*, 1970, **61**, 448–57.
36 Feughelman M, 'The mechanical properties of set wool fibres and the structure of keratin'. *J. Text. Inst.*, 1960, **51**, T589–600.
37 Hearle J W S, Chapman B M and Senior G S, 'The interpretation of the mechanical properties of wool', *Appl. Polymer Symp.*, No. 18, 1971, 775–94.
38 Feughelman M, 'Two-phase structure for keratin fibres', *Text. Res. J.*, 1959, **29**, 223–8.
39 Curiskis J I, 'A study of the micromechanics of fibrous reinforced composite materials using finite-element techniques', *PhD thesis*, University of New South Wales, 1978.
40 Curiskis J I and Feughelman M, 'Finite element analysis of the composite fibre, alpha keratin', *Text. Res. J.*, 1983, **53**, 271–4.
41 Chapman B M, 'A mechanical model for wool and other keratin fibres', *Text. Res. J.*, 1969, **39**, 1102–9.
42 Feughelman M and Haly A R, 'The mechanical properties of wool keratin and its molecular configuration', *Kolloid Z.*, 1960, **168**, 107–17.

43 Wortmann F-J and Zahn H, 'The stress–strain curve of α-keratin fibers and the structure of the intermediate filaments', *Text. Res. J.*, 1994, **64**, 737–43.
44 Feughelman M, 'A model for the mechanical properties of the α-keratin cortex', *Text. Res. J.*, 1994, **64**, 236–9.
45 Bendit E G, 'Quantitative X-ray diffraction of the α-β transformation in wool keratin', *Text. Res. J.*, 1960, **30**, 547–55.
46 Hearle J W S and Susutoglu M, 'Interpretation of the mechanical properties of wool fibres', *Proc. 7th Int Wool Text. Res. Conf.*, Tokyo, 1985, **1**, 214–23.
47 Bryson W G, Mastronarde D N, Caldwell J P, Nelson W G and Woods J L, 'High voltage microscopical imaging of the macrofibril ultrastructure reveals the three-dimensional spatial arrangement of intermediate filaments in Romney wool cortical cells – a causative factor in fibre curvature', *Proc. 10th Int. Wool Text. Res. Conf.*, Aachen, 2000 (on CD from DWI, Aachen).
48 Munro W A and Carnaby G A, 'Wool-fibre crimp. Part I: The effects of microfibrillar geometry', *J. Text. Inst.*, 1999, **90**, 123–36.
49 Horio M and Kondo T, 'Crimping of wool fibres', *Text. Res. J.*, 1953, **23**, 373–87.
50 Mercer E H, 'The heterogeneity of the keratin fibers', *Text. Res. J.*, 1953, **23**, 388–97.
51 Hearle J W S, 'Can genetic engineering enhance the miracle of wool? Part 3: Why worry about fibre strength?' *Text. Horizons*, 1997, August/September 12–16.
52 Hobbs R E, Overington M S, Hearle J W S and Banfield S J, Buckling of fibres and yarns within ropes and other assemblies, *J. Text. Inst.*, 2000, **91**, 335–58.
53 Lincoln B, 'The frictional properties of the wool fibre', *J. Text. Inst.*, 1954, **45**, T92–107.
54 Hearle J W S, 'The dielectric properties of fibre assemblies', *Text. Res. J.*, 1956, **26**, 108–11.
55 Hearle J W S, 'The electrical resistance of textile materials: IV. Theory', *J Textile Inst*, 1953, **44**, T177–98.
56 Hearle J W S, Grosberg P and Backer S, *Structural Mechanics of Fibers, Yarns and Fabrics*, Wiley-Interscience, New York, 1969.
57 Hearle J W S, Thwaites J J and Amirbayat J, *Mechanics of Flexible Fibre Assemblies*, Sijthoff & Noordhoff, Alphen an den Rijn, Netherlands, 1980.
58 Hearle J W S, 'Mechanics of yarns and nonwoven fabrics', in Chou T-W and Ko F K (editors) *Textile Structural Composites*, Elsevier, Amsterdam, 1989.
59 Kawabata S and Niwa M, 'Fabric performance in clothing and clothing manufacture', *J. Text. Inst.*, 1989, **80**, 19–51.
60 Hearle J W S and El-Sheikh A, 'The mechanics of wool yarns', *Proc. 3rd Int. Wool Text. Res. Conf.*, Paris, 1965, **IV**, 267–76.
61 Carnaby G A and Grosberg P, 'The tensile behaviour of staple-fibre yarns at small extensions', *J. Text. Inst.*, 1976, **67**, 299–308.
62 Carnaby G A and Grosberg P, 'The mechanics of the relaxation of wool carpet yarns. Part I: Theoretical analysis', *J. Text. Inst.*, 1977, **68**, 24–32.
63 Carnaby G A and Grosberg P, 'The mechanics of the relaxation of wool carpet yarns. Part II: Experimental evaluation of theory', *J. Text. Inst.*, 1977, **68**, 33–6.
64 Amirbayat J and Hearle J W S, 'The anatomy of buckling of textile fabrics', *J. Text. Inst.*, 1989, **80**, 52–70.
65 Munden D L, 'The geometry and dimensional properties of plain-knit fabrics', *J. Text. Inst.*, 1959, **50**, T448–71.

66 Chapman B M, 'A model for the crease recovery of fabrics', *Text. Res. J.*, 1974, **44**, 531–8.
67 Chapman B M, 'The relationship between single fibre bending behaviour and fabric wrinkle recovery', *Proc. 5th Int. Wool Text. Res. Conf.*, Aachen, 1975, **III**, 483–92.
68 Hearle J W S, 'A theory of the mechanics of needled fabrics', in Lennox-Kerr (editor), *Needle-felted Fabrics*, The Textile Trade Press, Manchester, 1972, 51–64.
69 Carnaby G A and Wood E J, 'The physics of carpets', *J. Text. Inst.*, 1989, **80**, 71–90.
70 Hearle JWS, Liu H, Tandon S K and Wood E J, 'Fibre Fatigue mechanisms in wool carpet near and the modelling of carpet durability', *Proc. 10th Int. Wool Text. Res. Conf.*, Aachen, 2000 (on CD from DWJ, Aachen).